Studies on Structural and Optical Properties of Pristine and Ni doped Zinc Oxide Nanorods

Dissertation Submitted to the

University of Kerala for the Partial Fulfilment of the Requirement

for the Award of The Degree of

BACHELOR OF SCIENCE

In

PHYSICS

By

ANANTHU S (REG.NO: 23019101021)

JYOTHI REKHAN (REG.NO: 23019101011)

Department of Physics

Bishop Moore College, Mavelikara

Affiliated to

UNIVERSITY OF KERALA, INDIA

Under the guidance of

Dr D Sajan

Head of The Department

Bishop Moore College, Mavelikara

Project report 2022

Studies on Structural and Optical Properties of Pristine and Ni doped Zinc Oxide Nanorods

Post Graduate and Research Department of Physics

Bishop Moore College, Mavelikara

Dissertation submitted to the University of Kerala in partial fulfilment for the degree of

B.Sc. in Physics

Name : **ANANTHU S (23019101021)**

JYOTHI REKHAN (23019101011)

Class : **BSc Physics**

Year : **2019-2022**

Year of Appearance : **2022**

CERTIFIED GENUINE

Signature of Lecture in charge:

Signature of Examiners: **1.**

2.

Date:

Estd. 1964

DEPARTMENT OF PHYSICS
BISHOP MOORE COLLEGE
Mavelikara, Kerala, India, 690110
Re-assessed and Re-accredited (Third Cycle) with 'A' Grade by NAAC
Supported by DST-FIST, DBT Star College & KSCSTE SARD Schemes

Dr.D.Sajan
Associate Professor
Head of the Department
Email: drsajanbmc@gmail.com
Phone: 9495043765

08 May 2022

Certificate

This is to certify that dissertation entitled ***"Studies on Structural and Optical Properties of Pristine and Ni doped Zinc Oxide Nanorods"*** is a record of original work carried out by **Ananthu S** (Reg. No: 23019101021) and **Jyothi Rekhan** (Reg. No: 23019101011) under my supervision and guidance during 2020-2022 in partial fulfillment of the requirement for the award of the degree of bachelor of science, under University of Kerala, Thiruvananthapuram. Neither this dissertation nor any part of it has been submitted for any degree or diploma to any institute or university in India or abroad.

Dr. D. Sajan

Supervising Teacher

Kallumala P.O, Mavelikara, Kerala- 690110,Kerala,India, Phone: +91-479 230 3260,Fax: +91-479 230 3260
Website :www.bishopmoorecollege.org, Email: hodbmcphysics@gmail.com

Declaration of Originality

We, **Jyothi Rekhan (Reg. No.23019101011),** and **Ananthu S (Reg. No.23019101021)** hereby declare that this dissertation entitled **"Studies on Structural and Optical Properties of Pristine and Ni Doped Zinc Oxide Nanorods"** represents our original work carried out as a Bachelor of Science students of University of Kerala and to the best of our knowledge, it contains no material previously published or written by another person, nor any material presented for the award of other degree or diploma of University of Kerala or any other institution. Any contribution made to this research by others, with whom we have worked at University of Kerala or elsewhere, is explicitly acknowledged in the dissertation. Work of other authors cited in this dissertation have been duly acknowledge under the section "Reference". We are fully aware that in case of non-compliance detected in future, the Senate of University of Kerala may withdraw the degree awarded to me on the basis of the present dissertation.

Jyothi Rekhan

Ananthu S

Acknowledgement

Foremost, we would like to express my sincere gratitude to our guide **Dr D Sajan, HOD, Bishop Moore College, Mavelikara** for his continuous support, patience, motivation, enthusiasm and most knowledge. He was always a source of inspiration to us. His guidance helped in all the time of research and writing this project. We could not imagine having a better advisor and mentor for our research. The work could not have been possible without his worthy suggestions and constant co-operation.

Our heart is fulfilled with deep sense of thankfulness and obeisance to our teachers for their valuable suggestions. We also express our thanks to all faculty members of Bishop Moore College, Mavelikara for their constant support.

Our sincere thanks and gratitude to **Ms. Anjana M P, Research Scholar, Department of Physics, Bishop Moore College, Mavelikara,** for her kind support during the project work. We are grateful for her inspiring and valuable suggestions during the entire period of our project work, which enabled us to complete the work successfully.

We are grateful to our parents for their love, prayers, caring and sacrifices. We also thank our friends for giving us strength.

Jyothi Rekhan

Ananthu S

Contents

ABSTRACT

Metal oxide nanoparticles are the potential candidates in nanoscience research area. According to the synthesis methods, precursors, conditions we can tune the properties of the nanomaterials. Here in the present work we prepared the Ni-doped zinc oxide nanoparticles using hydrothermal method. Structural analysis of prepared samples is characterized using X-ray diffraction studies and SEM analysis is used to analyze the morphology of the samples. Elemental compositions are identified using Energy Dispersive X-ray analysis. The optical properties of pure and doped materials are studied by using UV visible spectroscopy and energy band gap is also calculated for 3.02eV for pure zinc oxide and it decreases to 2.15Ev after Ni doping. Functional groups and vibrational bands are also identified using Ftir and Raman Spectroscopy.

CHAPTER 1

INTRODUCTION

1.0 Nanoscience

"Nanoscience" is the emerging science of objects that are intermediate in size between the largest molecules and the smallest structures that can be fabricated by current photolithography; that is, the science of objects with smallest dimensions ranging from a few nanometers to less than 100 nanometers [1-3]. Nanoscience is concerned with materials and systems whose structures and components exhibit novel and significantly improved physical, chemical and biological properties, phenomena and processes, because of their small nanoscale size. Structural features in the range of about 10 Å to 1000 Å, determine important changes as compared to the behavior of isolated molecules (10Å) or of bulk materials (>0.1 μm). Nanoscience aims to understand the novel properties and phenomena of nano-based entities. The linguistic form *nano* originates from the classical Latin *nanus* or its ancient Greek etonym *nanos* meaning "dwarf". In 1958, nano, together with giga, tera, and pico, was adopted in the newly formed International System of units. In 1974, Norio Taniguchi introduced the term nanotechnology at an engineering conference in Tokyo. Feynman's lectures or Norio Taniguchi's original use of the term "nanotechnology" are often cited as the starting points for the concept, scientists have long investigated nanoscale materials and wondered about the nature of materials on small length scales [4].

1.1 Nanotechnology

Nanotechnology can be understood as a technology of design, fabrication and applications of nanostructures and nanomaterials, as well as fundamental understanding of physical properties and phenomena of nanomaterials and nanostructures [4]. According to National Science Foundation and NNI, nanotechnology is the ability to understand, control, and manipulate matter at the level of individual atoms and molecules, as well as at the "supramolecular" level involving clusters of molecules (in the range of about 0.1 to 100 nm), in order to create materials, devices, and systems with fundamentally new properties and functions because of their small structure. [5]. Nanotechnology aims to gain control of structures and devices at the atomic, molecular and supramolecular levels, and to learn how to efficiently manufacture and use these devices.

The idea of nanotechnology started in the 1950s, though the name wasn't invented until 1974. In a way, though, nanotechnology has been around for centuries. After all, a lot of chemistry is about controlling nanoscale objects – atoms and molecules – and since ancient times, artists have used the special properties of gold and other metal nanoparticles to color glass, but without knowing about 'nanoparticles'. In recent years nanotechnology has become one of the most important and exciting forefront fields in Physics, Chemistry, Engineering and Biology. It shows great promise for providing us in the near future with many breakthroughs that will change the direction of technological advances in a wide range of applications. The WTEC study concluded that this technology has enormous potential to contribute to significant advances over a wide and diverse range of technological areas ranging from producing stronger and lighter materials, to shortening the delivery time of nano structured pharmaceuticals to the body's circulatory system, increasing the storage capacity of magnetic tapes, and providing faster switches for computers. Recommendations made by this and subsequent panels have led to the appropriation of very high levels of finding in recent years. The research area of nanotechnology is interdisciplinary, covering a wide variety of subjects ranging from the chemistry of the catalysis of nanoparticles, to the physics of the quantum dot laser [6]

1.2 History of Nanoscience and Nanotechnology

It is not clear when humans first began to take advantage of nanosized materials. It is known that in the fourth-century A.D. Roman glassmakers were fabricating glasses containing nanosized metals. An artifact from this period called the Lycurgus cup resides in the British Museum in London. The cup, which depicts the death of King Lycurgus, is made from soda lime glass containing silver and gold nanoparticles. The color of the cup changes from green to a deep red when a light source is placed inside it. The great varieties of beautiful colors of the windows of medieval cathedrals are due to the presence of metal nanoparticles in the glass [6].

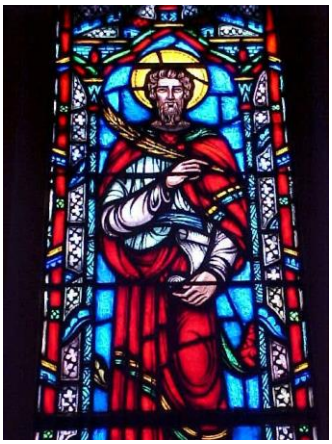

Figure 1.0 Lycurgus Cup (British Museum; AD fourth century) **Figure 1.1** Medieval stained glass

In 1867, James Clerk Maxwell put forward some of the important and leading concept about nanotechnology. Later the concept of a ‘‘nanometer’’ was first proposed by Richard Zsigmondy, the 1925 Nobel Prize Laureate in chemistry. He coined the term nanometer explicitly for characterizing particle size and he was the first to measure the size of particles such as gold colloids using a microscope. Modern nanotechnology was the brain child of Richard Feynman, the 1965 Nobel Prize Laureate in physics. During the 1959 American Physical Society meeting at Caltech, he presented a lecture titled, ‘‘There’s Plenty of Room at the Bottom’’, in which he introduced the concept of manipulating matter at the atomic level. This novel idea demonstrated new ways of thinking and Feynman’s hypotheses have since been proven correct. It is for these reasons that he is considered the father of modern nanotechnology. Almost 15 years after Feynman’s lecture, a Japanese scientist, Norio Taniguchi, was the first to use ‘‘nanotechnology’’ to describe semiconductor processes that occurred on the order of a nanometer. He advocated that nanotechnology consisted of the processing, separation, consolidation, and deformation of materials by one atom or one molecule. The golden era of nanotechnology began in the 1980s when Kroto, Smalley, and Curl discovered fullerenes and Eric Drexler of Massachusetts Institute of Technology (MIT) used ideas from Feynman’s ‘‘There is Plenty of Room at the Bottom’’ and Taniguchi’s term nanotechnology in his 1986 book titled, ‘‘Engines of Creation: The Coming Era of Nanotechnology.’’ Drexler proposed the idea of a nanoscale ‘‘assembler’’ which would be able to build a copy of itself and of other items of arbitrary complexity. Drexler’s vision of nanotechnology is often called ‘‘molecular nanotechnology.’’ The science of nanotechnology was advanced further when Iijima, another Japanese scientist, developed carbon nanotubes [7].

The beginning of the 21st century saw an increased interest in the emerging fields of nanoscience and nanotechnology. In the United States, Feynman's stature and his concept of manipulation of matter at the atomic level played an important role in shaping national science priorities. President Bill Clinton advocated for funding of research in this emerging technology during a speech at Caltech on January 21, 2000. Three years later, President George W. Bush signed into law the 21st Century Nanotechnology Research and Development Act. The legislation made nanotechnology research a national priority and created the National Technology Initiative (NNI) [7].

Today, the NNI is managed within a framework at the top of which is the President's Cabinet-level National Science and Technology Council (NSTC) and its Committee on Technology. The Committee's Subcommittee on Nanoscale Science, Engineering, and Technology (NSET) is responsible for planning, budgeting, implementation, and review of the NNI and is comprised of representatives from 20 US departments and independent agencies and commissions [7].

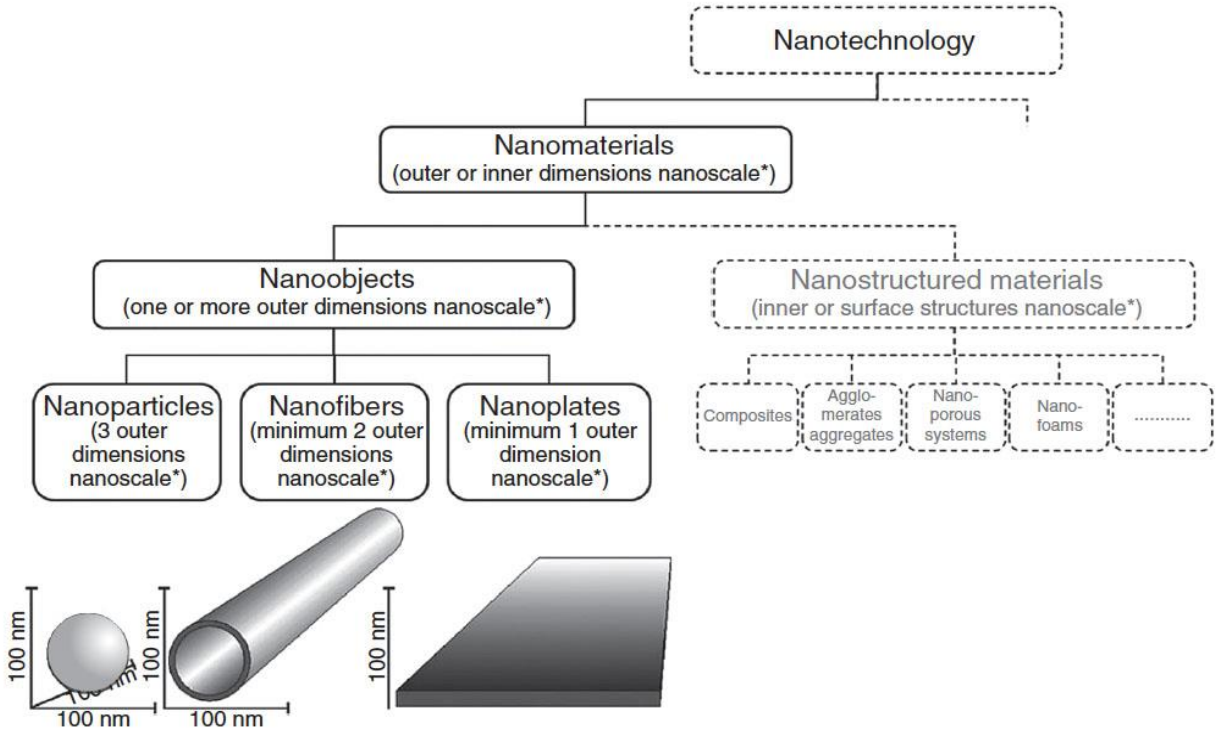

Figure 1.2 Classification of Nanotechnology

1.3 Nanoparticles

A nanoparticle or ultrafine particle is usually defined as a particle of matter that is between 1 and 100 nanometres (nm) in diameter. The term is sometimes used for larger particles, up to 500 nm, or fibers and tubes that are less than 100 nm in only two directions. At the lowest range, metal particles smaller than 1 nm are usually called atom clusters instead. Nanoparticles are usually distinguished from microparticles (1-1000 μm), "fine particles" (sized between 100 and 2500 nm), and "coarse particles" (ranging from 2500 to 10,000 nm), because their smaller size drives very different physical or chemical properties, like colloidal properties and optical or electric properties. Being more subject to the Brownian motion, they usually do not sediment, like colloidal particles that conversely are usually understood to range from 1 to 1000 nm. Being much smaller than the wavelengths of visible light (400-700 nm), nanoparticles cannot be seen with ordinary optical microscopes, requiring the use of electron microscopes or microscopes with laser. For the same reason, dispersions of nanoparticles in transparent media can be transparent, whereas suspensions of larger particles usually scatter some or all visible light incident on them. Nanoparticles also easily pass through common filters, such as common ceramic candles, so that separation from liquids requires special nanofiltration techniques.

The properties of nanoparticles often differ markedly from those of larger particles of the same substance. Since the typical diameter of an atom is between 0.15 and 0.6 nm, a large fraction of the nanoparticle's material lies within a few atomic diameters from its surface. Therefore, the properties of that surface layer may dominate over those of the bulk material. This effect is particularly strong for nanoparticle dispersed in a medium of different composition, since the interactions between the two materials at their interface also becomes significant [9] .

1.4 Classification of Nanomaterials based on origin

1.4.1 Natural Nanomaterials:

Natural nanomaterials are produced in nature either by biological species or through anthropogenic activities. The production of artificial surfaces with exclusive micro and nanoscale templates and properties for technological applications are readily available from natural sources. Naturally occurring nanomaterials are present through the Earth’s spheres (i.e., in the

hydrosphere, atmosphere, lithosphere and even in the biosphere), regardless of human actions. Earth is comprised of nanomaterials that are naturally formed and are present in the Earth's spheres, such as the atmosphere, which includes the whole of troposphere, the hydrosphere, which includes oceans, lakes, rivers, groundwater and hydrothermal vents, the lithosphere, which is comprised of rocks, soils, magma or lava at particular stages of evolution and the biosphere, which covers micro-organisms and higher organisms, including humans [9].

1.4.2 Synthetic Nanomaterials:

Synthetic (engineered) nanomaterials are produced by mechanical grinding, engine exhaust and smoke, or are synthesized by physical, chemical, biological or hybrid methods. The question of risk assessment strategies has arisen in recent times as there is increased fabrication and subsequent release of engineered nanomaterials as well as their usage in consumer products and industrial applications. These risk assessment strategies are highly helpful in forecasting the behavior and fate of engineered nanomaterials in various environmental media. The major challenge among engineered nanomaterials is whether existing knowledge is enough to forecast their behavior or if they exhibit a distinct environment related behavior, different from natural nanomaterials. Currently, different sources related to potential applications are used for the production of engineered NMs [10].

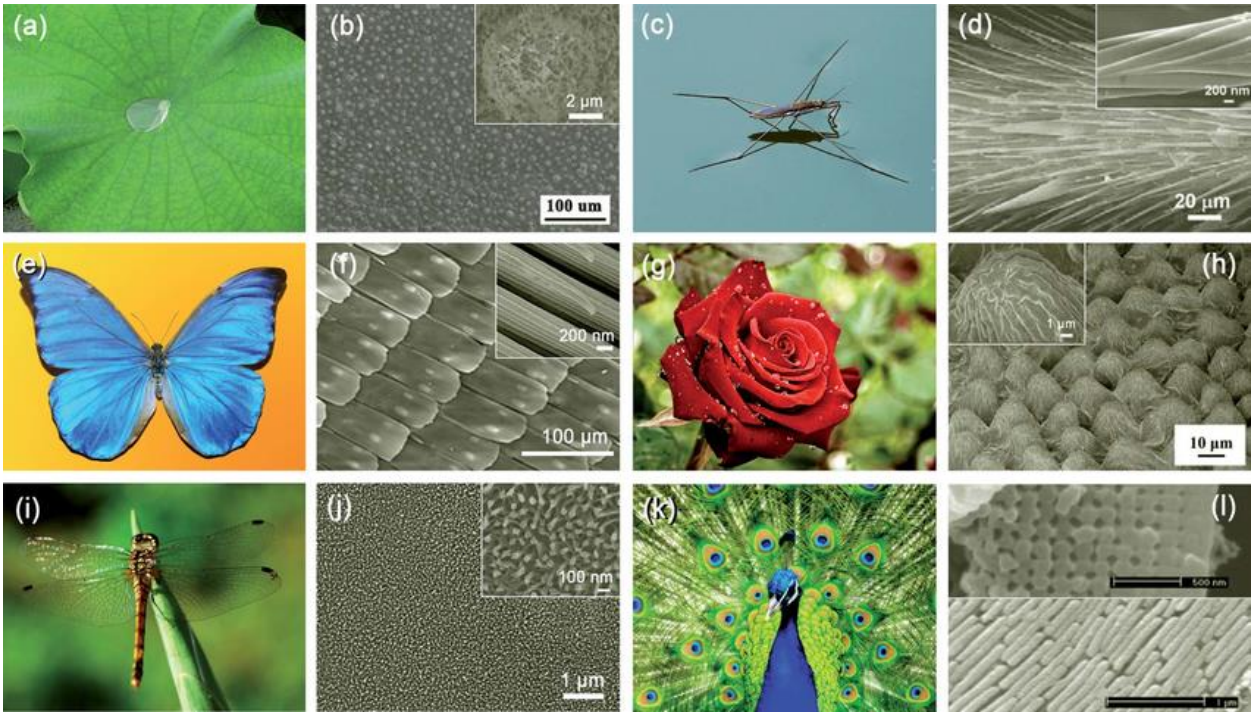

Figure 1.3 (a) Photograph of a lotus leaf; (b) SEM image of the lotus leaf surface. (c) Photograph of a water strider. (d) SEM image of the water strider leg (e) Photograph of a Morpho. (f) SEM image of the hierarchical micro-and nanostructures on the surface of butterfly wings (g) Photograph of a red rose, water droplets can pin to the rose petals surface. (h) SEM image of a rose petals surface. (i) Photograph of a dragonfly. (j) SEM image of a dragonflys wing. (k) Photograph of a peacock feathers. (l) SEM images of the transverse (top) and longitudinal (bottom) cross-sections of the cortex of the green barbule.

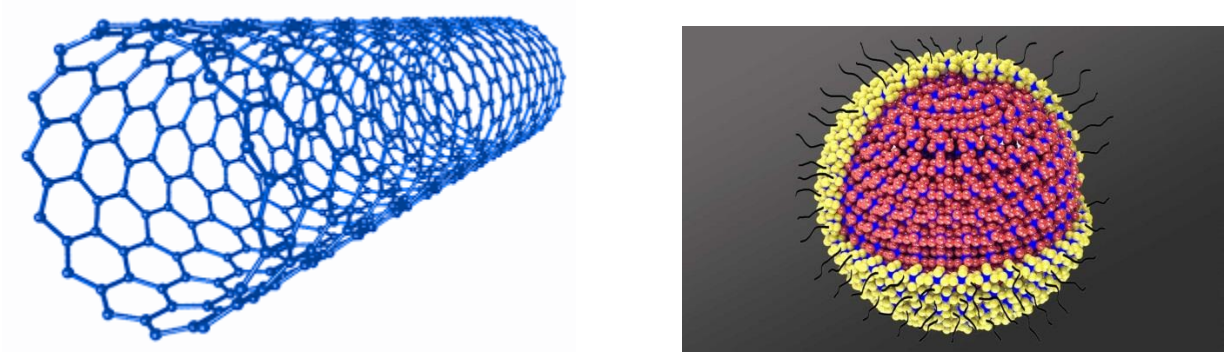

Figure 1.4 Carbon Nanotube and quantum dots

1.5 Classification of Nanomaterials based on the number of dimensions

Nanostructured materials are classified as: zero-dimensional (0D (1D), two-dimensional (2D) and three-dimensional (3D) nanomaterials**.**

1.5.1 Zero-dimensional nanomaterials:

Here, all dimensions (x, y, z) are at nanoscale, i.e., no dimensions are greater than 100 nm, electrons in 0D NMs are entrapped in a dimensionless space. It includes graphene quantum dots (GQDs), carbon quantum dots (CQDs), fullerenes, inorganic quantum dots (QDs), magnetic nanoparticles (MNPs), noble metal nanoparticles, upconversion nanoparticles (UCNPs) and polymer dots (Pdots)

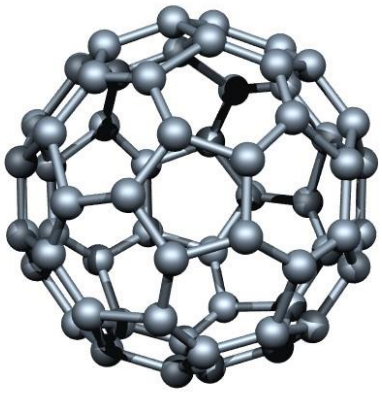

Figure 1.6 Fullerene

1.5.2 One-dimensional nanomaterials:

Here, two dimensions (x, y) are at nanoscale and the other is outside the nanoscale. This leads to needle shaped nanomaterials. Electrons are confined within two dimensions, indicating electrons cannot move freely. These 1D nanomaterials can be amorphous or crystalline; single or poly crystalline, and metallic, ceramic, or polymeric. Examples include nanotube, nanofiber, nanowire and nanorod, and nanofilaments. [11]

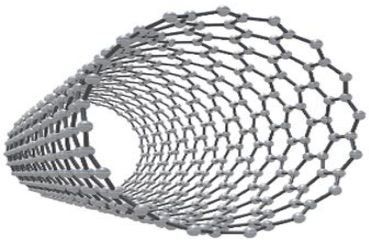

Figure 1.7 Carbon Nanotube

1.5.3 Two-dimensional nanomaterials:

Here, one dimension (x) is at nanoscale and the other two are outside the nanoscale. The 2D nanomaterials exhibit plate like shapes. It includes nanofilms, nanolayers and nano coatings with nanometer thickness.

Examples include graphene, hexagonal boron nitride (hBN), and metal dichalcogenides (MX_2) [11].

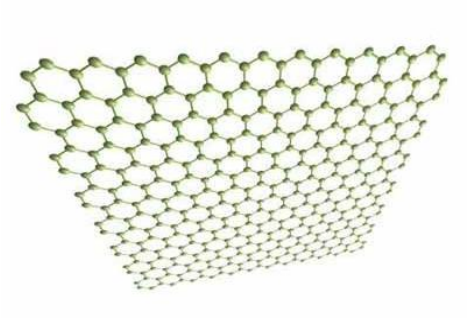

Figure 1.8 Graphene

1.5.4 Three-dimensional nanomaterials:

These are the nanomaterials that are not confined to the nanoscale in any dimension. These materials have three arbitrary dimensions above 100 nm. The bulk (3D) nanomaterials are composed of a multiple arrangement of nano size crystals in different orientations. It includes

dispersions of nanoparticles, bundles of nanowires and nanotubes as well as multinanolayers (polycrystals) in which the 0D, 1D and 2D structural elements are in close contact with each other and form interfaces [11].

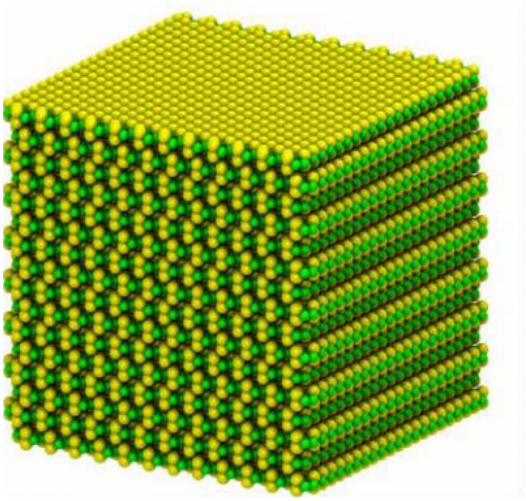

Figure 1.9 Bulk Nanomaterial

1.6 Classification of Nanomaterials based on Materials

1.6.1 Carbon-Based Nanomaterials

These types of nanomaterials are made up of carbon content and have various morphologies. The carbon-based nanomaterials can be hollow tubes or spheres, carbon nanofibers, Fullerenes, and graphene. The different methods used for the synthesis of carbon-based nanomaterials include chemical vapor deposition (CVD), arc discharge, and laser ablation.

(a) Fullerenes: Fullerenes (C60) are spherical carbon molecules made up of carbon atoms arranged in sp2 hybridization. Fullerenes contain 28–1500 carbon atoms arranged in spherical structures with a diameter of up to 8.2nm for a single-layered fullerene and 4–36nm for a multi-layered fullerene.

(b) Graphene: This is the carbon-containing network. The arrangement of carbon atoms forms a hexagonal pattern in the graphene network and makes two-dimensional planar surfaces. The thickness of a two-dimensional sheet is about 1–2nm.

(c) Carbon nano tubes (CNTs): These are nanofoils made up of carbon-containing graphene. The carbon atoms are arranged in honeycomb lattice in carbon nanotubes and form hollow cylinders of 0.7nm diameter for a single-layered CNT and about 100nm for a multi-layered CNT. The length of CNT varies from a few μm to a few mm.

(d) Carbon nanofibers: The graphene nanofoils used in the production of carbon nanofibers are the same as CNTs but the structure is different. The graphene molecules are arranged in cone or cup form rather than the regular cylindrical tubes of CNTs.

(e) Carbon black: This is an amorphous nanomaterial made up of carbon atoms that are arranged in a spherical shape with diameters from 20 to 70nm. The carbon black particle–particle interaction is so high that they bind with each other and form aggregates around 500nm.

1.6.2 Inorganic-Based Nanomaterials

It is these nanomaterials that make up metals and metal oxides. They can be synthesized from metals such as Ag, Au, and Fe: and the metal oxides are TiO2, ZnO, and MnO2. Semiconductor nanomaterials are also synthesized from silicon and ceramic materials.

1.6.3 Organic-Based Nanomaterials

The organic-based nanomaterials are made up of organic matter other than carbon and inorganic material. The synthesis of these nanomaterials is through self-assembly or transformation from organic matter into the desired structure. The noncovalent (weak) interaction applies in these types of materials.

1.7 Composite-Based Nanomaterials

Composite nanomaterials are made up of one more layer of nanoparticles. These nanomaterials are combined with other nanoparticles, bulk materials, or more complex materials like metal frameworks. The composites may be made up of many types of materials such as metal, ceramic, organic, inorganic, carbon-based, or bulk polymers. These materials have different morphologies depending on the synthesis and required properties for the desired applications [12].

1.7.1 Nanocomposites

Nanocomposite is a multiphase solid material where one of the phases has one, two or three dimensions of less than 100 nanometers (nm) or structures having nano-scale repeat distances between the different phases that make up the material. The idea behind Nanocomposite is to use building blocks with dimensions in nanometre range to design and create new materials with unprecedented flexibility and improvement in their physical properties. In the broadest sense this definition can include porous media, colloids, gels and copolymers, but is more usually taken to mean the solid combination of a bulk matrix and nano-dimensional phase(s) differing in properties due to dissimilarities in structure and chemistry. The mechanical, electrical, thermal, optical, electrochemical, catalytic properties of the nanocomposite will differ markedly from that of the component materials [13]

Nanoclay-based polymeric nanocomposites are among the first composites to be launched in the market as improved packaging tools. They have been developed from thermoplastic polymer fabricated with clay nanoparticles, which include nylons, polyamides, polystyrene, polyolefin, polyurethane, epoxy resins, polyimides, and polyethylene terephthalate. These are often used for nanoclay-based multilayer film packaging of beverages, beers, carbonated drinks, and edible oils. Nanocomposites are found in nature, for example in the structure of the abalone shell and bone. The use of nanoparticle-rich materials long predates the understanding of the physical and chemical nature of these materials. In mechanical terms, nanocomposites differ from conventional composite materials due to the exceptionally high surface to volume ratio of the reinforcing phase and/or its exceptionally high aspect ratio.[13]

1.8 Synthesis Methods of Nanomaterials

The synthesis of nanomaterials is a key to the future success of this new technology and in principle; the approaches to the synthesis of nanomaterials can be divided into two main classes: Top-down approaches and bottom-up approaches.

1.8.1 Top-down approach

Top-down approach involves the breaking down of the bulk material into nanosized structures or particles. Top-down synthesis techniques are extension of those that have been used for

producing micron sized particles. Top-down approaches are inherently simpler and depend either on removal or division of bulk material or on miniaturization of bulk fabrication processes to produce the desired structure with appropriate properties. The biggest problem with the top-down approach is the imperfection of surface structure. For example, nanowires made by lithography are not smooth and may contain a lot of impurities and structural defects on its surface. Examples of such techniques are high-energy wet ball milling, electron beam lithography, atomic force manipulation, gas-phase condensation, aerosol spray, etc. [14].

Many top-down mechanical methods are utilized by industry. Thermal methods form a nebulous category and we try and focus on those that provide heat to a fabrication process. Of these, electrospinning is a means to form nano thread materials. High energy methods are those that require an excessive input of energy– whether in the form of heat, electricity or solar energy. Arc discharge was the first controlled means of making carbon nanotubes. Laser ablation and solar flux also work well. The problem is control of quality and potential upscale. Lithographic methods, as we all know quite well, although energy intensive and requiring expensive equipment and facilities are top-down methods capable of producing for the most part micron-sized features [14].

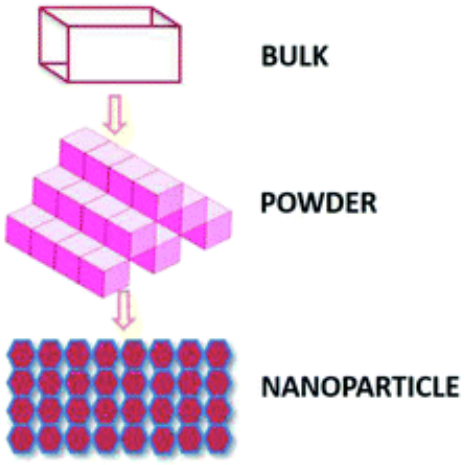

Figure 1.10 Top-Down Approach

1.8.1.1 Examples for top-down approach

❖ **Ball milling**

Ball milling is a mechanical technique that is broadly used to grind powders into fine particles . The reactants are generally broken apart using solvent molecules in the traditional method; but in ball milling, reactants are broken by using mechanical forces. The term mechanochemistry has been introduced very recently. The use of ball milling in the synthesis and reactions of organic compounds have been published in many review articles. The application of solvent-free ball milling in organic synthesis is relatively rare. However, in the last decade, this technique has attracted growing interest because of its simplicity, low cost, and environment friendliness, as well as its capability to achieve very high yields. On the basis of these aspects, research will definitely increase in future in basic and applied science fields [15].

Fig 1.11 Ball milling process

❖ **Electron Beam Lithography**

Electron-beam lithography (often abbreviated as e-beam lithography, EBL) is the practice of scanning a focused beam of electrons to draw custom shapes on a surface covered with an electron-sensitive film called a resist (exposing). The electron beam changes the solubility of the

resist, enabling selective removal of either the exposed or non-exposed regions of the resist by immersing it in a solvent (developing). The purpose, as with photolithography, is to create very small structures in the resist that can subsequently be transferred to the substrate material, often by etching. The primary advantage of electron-beam lithography is that it can draw custom patterns (direct-write) with sub-10 nm resolution. This form of maskless lithography has high resolution and low throughput, limiting its usage to photomask fabrication, low-volume production of semiconductor devices, and research and development [16].

Fig 1.12 Electron beam lithography

❖ **Gas phase condensation**

Gas-phase synthesis characterizes a class of bottom-up methods for producing multifunctional nanoparticles (NPs) from individual atoms or molecules. This review aims to summarize recent achievements using this approach, and compare its potential to other physical or chemical NP fabrication techniques. More specifically, emphasis is given to magnetron-sputter gas-phase condensation, since it allows for flexible growth of complex, sophisticated NPs, owing to the fast kinetics and non-equilibrium processes it entails. Nanoparticle synthesis is decomposed into four stages, i.e., aggregation, shell-coating, mass-filtration, and deposition. We present the formation of NPs of various functionalities for different applications, such as magnetic, plasmonic, catalytic and, gas-sensing, emphasizing on the primary dependence of each type on a different stage of the fabrication process, and their resultant physical and chemical properties [17].

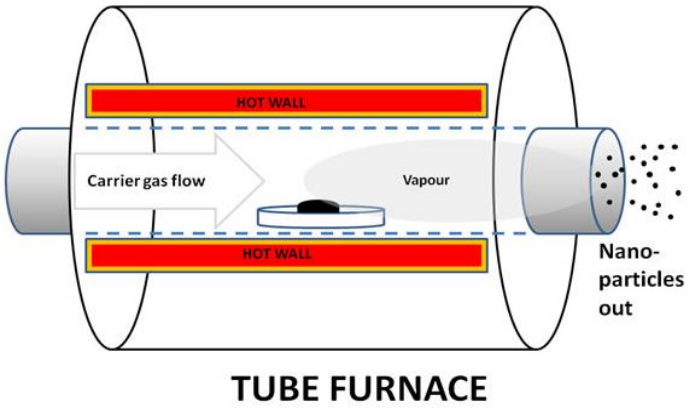

Fig 1.13 Gas phase synthesis

1.8.2 Bottom-up Approach

The alternative approach, which has the potential of creating less waste and hence the more economical, is the 'bottom- up'. Bottom-up approach refers to the buildup of a material from the bottom: atom-by-atom, molecule-by-molecule, or cluster-by cluster. Many of these techniques are still under development or are just beginning to be used for commercial production of nanopowders. Oraganometallic chemical route, revere-micelle route, sol-gel synthesis, colloidal precipitation, hydrothermal synthesis, template assisted sol-gel, electrodeposition etc, are some of the well- known bottom–up techniques reported for the preparation of luminescent nanoparticals [14].

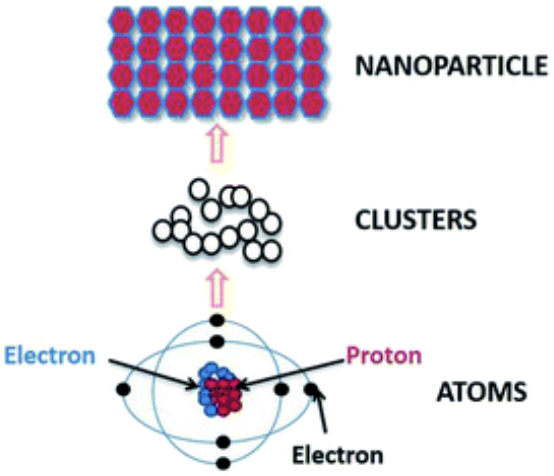

Figure 1.14 Bottom-Up Approach

1.8.2.1 Examples for Bottom-up approach

❖ **Hydrothermal method**

Hydrothermal method is a standard preparation route, especially for powdery nanostructure. Hydrothermal synthesis refers to the heterogeneous reactions for synthesizing inorganic materials in aqueous media above ambient temperature and pressure. In this case, an aqueous mixture of precursors is heated in a sealed stainless-steel autoclave above the boiling point of water, and consequently the pressure within the reaction autoclave is dynamically increased above atmospheric pressure. This effect of high temperature and pressure provides a one step process to produce highly crystalline materials without the need of post annealing treatment. The hydrothermal synthesis could obtain magnetic nanomaterials with very high crystallinity due to their high temperature and high-pressure reaction conditions. Hydrothermal method has several advantages such as low cost, easy experimental setup, and high yield.

As a result of the main thermodynamic and kinetic features of the hydrothermal process, the main advantages of the hydrothermal synthesis are:

- One step process for powder synthesis or oriented ceramic films.
- Minimized consumption of energy, particularly for complex and doped oxides.
- Products with much high homogeneity than solid state processing.
- Products with higher density than gas or vacuum processing.
- One of the few methods enabling for obtaining of controlled doped or complex material system.

Fig 1.15: The hydrothermal reaction set up and the Teflon jar and the stainless-steel autoclave with screws

❖ **Sol-gel Synthesis**

The sol-gel process is a more chemical method (wet chemical method) for the synthesis of various nanostructures, especially metal oxide nanoparticles. In this method, the molecular precursor (usually metal alkoxide) is dissolved in water or alcohol and converted to gel by heating and stirring by hydrolysis/alcoholysis. Since the gel obtained from the hydrolysis/alcoholysis process is wet or damp, it should be dried using appropriate methods depending on the desired properties and application of the gel. For example, if it is an alcoholic solution, the drying process is done by burning alcohol. After the drying stage, the produced gels are powdered and then calcined. The sol-gel method is a cost-effective method and due to the low reaction temperature there is good control over the chemical composition of the products. The sol-gel method can be used in the process of making ceramics as a molding material and can be used as an intermediate between thin films of metal oxides in various applications. The materials obtained from the sol-gel method are used in various optical, electronic, energy, surface engineering, biosensors, and pharmaceutical and separation technologies (such as chromatography). The sol-gel method is a conventional and industrial method for the synthesis of nanoparticles with different chemical composition. The basis of the sol-gel method is the production of a homogeneous sol from the precursors and its conversion into a gel. The solvent in the gel is then removed from the gel structure and the remaining gel is dried. The properties of the dried gel depend significantly on the drying method. In other words, the “removing solvent method” is selected according to the application in which the gel will be used. Dried gels in various ways are used in industries such as surface coating, building insulation, and the production of special clothing. It is worth mentioning that, by grinding the gel by special mills, it is possible to achieve nanoparticles[18].

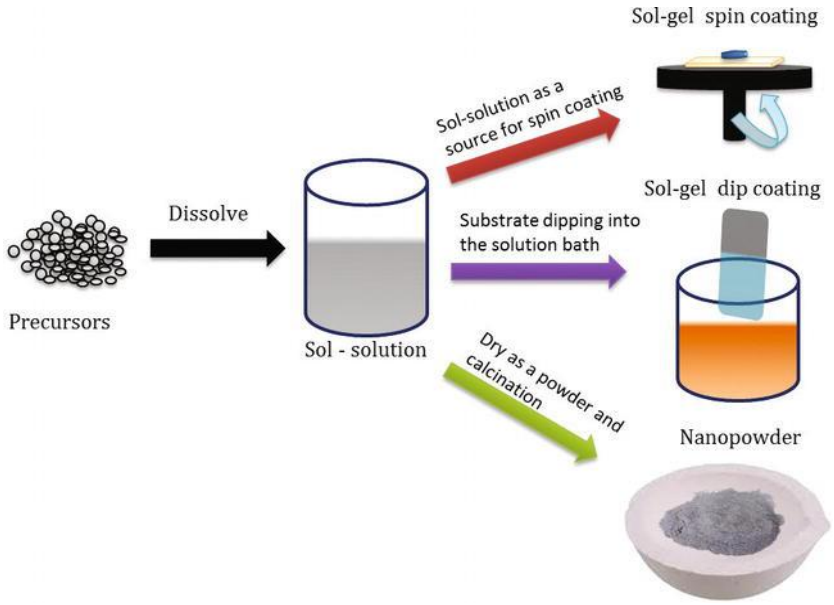

Fig 1.16 Sol gel synthesis

❖ Electrodeposition

Electrodeposition is a flexible low-cost method of fabrication of a wide variety of two- and three-dimensional materials such as coatings and films. The principles of the electrodeposition process are based on principles of electrochemical phenomena associated with the reduction or deposition of electroactive and accompanying species on the cathode surface. This would make the electrodeposition process more controllable if one considers the electrochemical principles into account for target purposes and applications. However, many empirical factors in designing and controlling of electrodeposition process exist. Anticorrosion coatings have been a major part of corrosion protection tools employed for years. Electrodeposition is one successful method to fabricate coatings. Thanks to remarkable advances in nanoscience and nanotechnology and exotic effects of the nanoscale size on properties and functionalities of materials, electrodeposition of nanocoatings has become an interesting subject of research recently. In this chapter, the electrodeposition of anticorrosion nanocoatings is described. After a brief overview of the electrodeposition, two types of nanocoatings including nanocomposites and nanocrystalline, their electrodeposition principles, and corrosion behavior based on conventional electrochemical studies are explained[19].

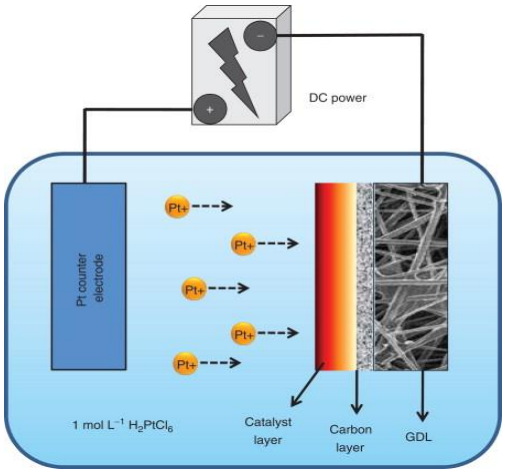

Fig1.17 Electrodeposition method

1.9 Zinc Oxide

The Zinc Oxide (ZnO) is n-type and wide band gap (3.37 eV) semiconductor material with a free-exciton binding energy (60 MeV) at room temperature. The ZnO is II-VI semiconductor as zinc and oxygen belong to the IInd group and VIth group of the periodic table respectively. ZnO has three main crystalline forms, such as wurtzite, rocksalt and cubic zinc. Under general conditions, ZnO has a hexagonal wurtzite structure and is stable under thermodynamic conditions. It has attracted a series of research activities for its exclusive optical and piezoelectric properties and its versatile applications in transparent electronics , piezoelectric devices , ultraviolet (UV) light, dye-sensitized solar cell , photocatalyst , gas sensors , and others. Due to large exciton binding energy, ZnO is an attractive material for the fabrication of light emitting device in the ultraviolet (UV) region. It is optically transparent material in the visible light region with high conductivity . The lack of center of symmetry in the structure of wurtzite ZnO possess a strong pyroelectric and piezoelectric properties, useful for manufacturing the piezoelectric sensor. ZnO is used in the invisible thin film transistor (TFT) due to its greater mobility of field effect than the silicon-based TFT [20][21].

1.9.1 ZnO Semiconductor

ZnO is an important II-VI compound semiconductor. These semiconductors are formed by combining two elements from II and VI groups of the periodic table respectively] due to its wide band gap of about 3.3 eV (Huang *et al.* 2001) and large exciton binding energy of 60 MeV (Law

et al. 2005) at room temperature. ZnO, a material with ubiquitous applications in piezoelectric transducers, varistors and as transparent electrodes is fast becoming one of the most studied materials mostly to the seminal work by Dietl *et al.* who predicted ferromagnetic ground state of Zn□□xMnxO with x = 5%. ZnO is one of the most important materials that we come across in our day-to-day lives. It has a hexagonal lattice belonging to the space group P63mc and is characterized by two interconnecting sublattices of Zn2+ and O2- such that each Zn ion is

surrounded by oxygen tetrahedra and vice-versa. ZnO crystallizes in three forms zinc blende, wurtzite and rarely cubic rocksalt structures. The thermodynamically stable phase is wurtzite and thus most common at ambient conditions. Different techniques such as pulsed laser deposition, sputtering, thermal evaporation, condensation, solid state reaction and chemical methods have been employed to fabricate such nanostructures. It has several favorable optical electrical and magnetic properties which are used in solar cells (Yoo *et al.* 2005) UV photodetectors (Jeong *et al.* 2004) gas sensors (Xu *et al.* 2006), photocatalytic activities (Park and Kang 1997; Szabo *et al.* 2004), LEDs and photonic applications. One of the key requirements for many of these applications is the doping of ZnO with various elements for enhancing and controlling its electrical and optical properties. Dietl *et al.* (2000) have predicted the origin of ferromagnetism in ZnO at room temperature on the incorporation of dilute amount of transition metal. The Crystal structure of Zno Rocksalt, Zincblende, Wurtzite given in Figure 1.18.

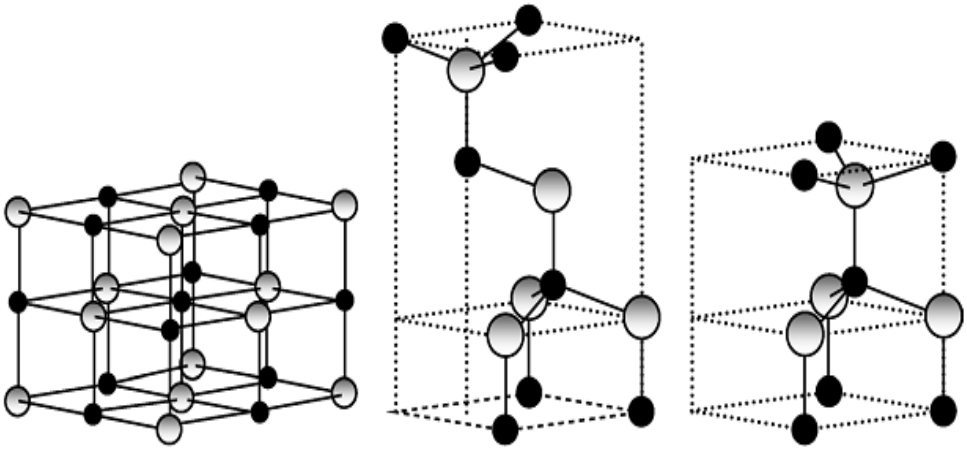

(a) (b) (c)

Figure 1.18 Crystal structure of Zno (a) Rocksalt, (b) Zincblende and (c) Wurtzite

1.9.2 Crystal structure of ZnO

Crystal structure is a unique arrangement of atoms or molecules in a crystalline liquid or solid. A crystal structure is composed of a pattern, a set of atoms arranged in a particular way, and a lattice exhibiting long-range order and symmetry. Patterns are located upon the points of a lattice, which is an array of points repeating periodically in three dimensions. The points can be thought of as forming identical tiny boxes, called unit cells, that fill the space of the lattice. A crystal's structure and symmetry play a role in determining many of its physical properties, such as cleavage, electronic band structure, and optical transparency. The crystal structure has a three dimensional shape. Most of the II-VI semiconductor crystallizes in either cubic zinc blende or hexagonal wurtzite structure. Zinc oxide is a white to yellow colored powder or crystal. ZnO crystallizes in three forms zinc blende, wurtzite and rarely cubic rocksalt structures. The thermodynamically stable phase is wurtzite and thus most common at ambient conditions. The zinc blende form can be stabilized by growing ZnO on substrates with cubic lattice structure. In both cases, the zinc and oxide are tetrahedral and at moderate external hydrostatic pressure it can be transformed to rocksalt structure.

Wurtzite Structure

The wurtzite structure is considered as closed packed hexagonal structures. The structure is made up of two interpenetrating hexagonal close packed (hcp) sublattices, each of which consist of one type of atom displaced with respect to each other along the three fold c-axis by the amount of U=3/8(U=length of the bond parallel to the c axis, in units of c). Each sublattice includes four atoms per unit cell and every atom of one kind is surrounded by four atoms of the other kind which are coordinated at the edges of a tetrahedron. In a ZnO the wurtzite structure deviates from its position by changing the c/a ratio or the u value. The representation for the crystal structure of wurtzite is shown in Figure1.19.

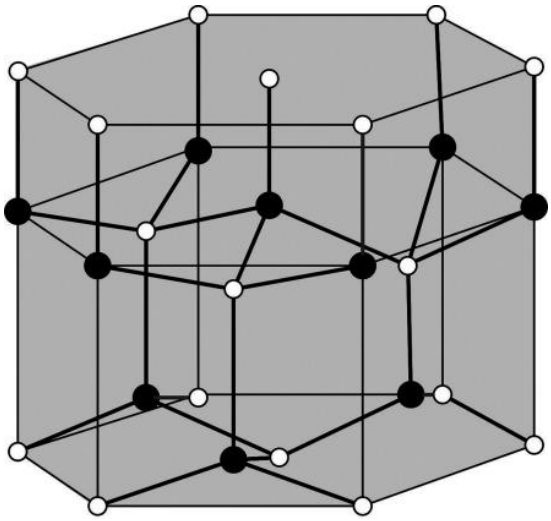

Figure 1.19 Crystal structure of Zno

Each Zn atom is tetrahedrally surrounded by four oxygen atoms. The wurtzite structure was arranged with alternating diatomic close packed (001) planes. In the wurtzite structure each atom has 12 nearest neighbours and the atoms fill 74.04% of the available space. The wurtzite structure is non-centrosymmetric. The zinc blende and wurtzite structures are very similar. The zinc blende structure consists of triangularly arranged atoms in the close packed planes and its stacking sequence is represented by the ABCABCABCABC repeating units along the (111) direction

This structure is called face centered cubic structure (FCC). Because of the tetrahedral co-ordination the four nearest neighbors and the 12 next nearest neighbors have the same bond length and the atoms fill 74.04% of the available space.

Like other II-VI semiconductors, wurtzite ZnO can be transformed to the rock salt structure at relatively external hydrostatic pressure. The reason for the transformation is that the reduction of the lattice dimensions causes the interionic coulomb interaction to favor the ionicity more over the covalent nature. However the rock salt structure cannot be stabilized by the epitaxial growth. Also the crystal structure exhibits polarity.

1.9.3 Defects In ZnO

Crystalline solids exhibit a periodic crystal structure. The positions of atoms or molecules occur on repeating fixed distances, determined by the unit cell parameters. However, the arrangement of atom or molecules in most crystalline materials is not perfect. The regular patterns are interrupted by crystallographic defects. All crystals have some defects. Zinc oxide is a transparent semiconductor that could prove to be a versatile material for fabricating light-emitting diodes and transparent electrodes. Yet controlling its conductivity remains a challenge. Defects contribute to the mechanical properties of metals. There are basic classes of crystal defects.

- Point defects, which are places where an atom is missing or irregularly placed in the lattice structure. Point defects include lattice vacancies, self-interstitial atoms, substitution impurity atoms, and interstitial impurity atoms.
- Linear defects, which are groups of atoms in irregular positions. Linear defects are commonly called dislocations.
- Planar defects, which are interfaces between homogeneous regions of the material. Planar defects include grain boundaries, stacking faults and external surfaces

Point defects are where an atom is missing or is in an irregular place in the lattice structure and is shown in Figure 1.15. Point defects include self interstitial atoms, interstitial impurity atoms, substitutional atoms and vacancies. A self interstitial atom is an extra atom that has crowded its way into an interstitial void in the crystal structure. A substitutional impurity atom is an atom of a different type than the bulk atoms, which has replaced one of the bulk atoms in the lattice. Substitutional impurity atoms are usually close in size to the bulk atom. Larger defects in an ordered structure are usually considered dislocation loops. For historical reasons, many point defects, especially in ionic crystals, are called centers, for example a vacancy in many ionic solids is called a luminescence center, a color center, or F-center. These dislocations permit ionic transport through crystals leading to electrochemical reactions. Vacancies are empty spaces where an atom should be, but is missing. They are common, especially at high temperatures when atoms are frequently and randomly change their positions leaving behind empty lattice sites. In most cases diffusion can only occur because of vacancies.

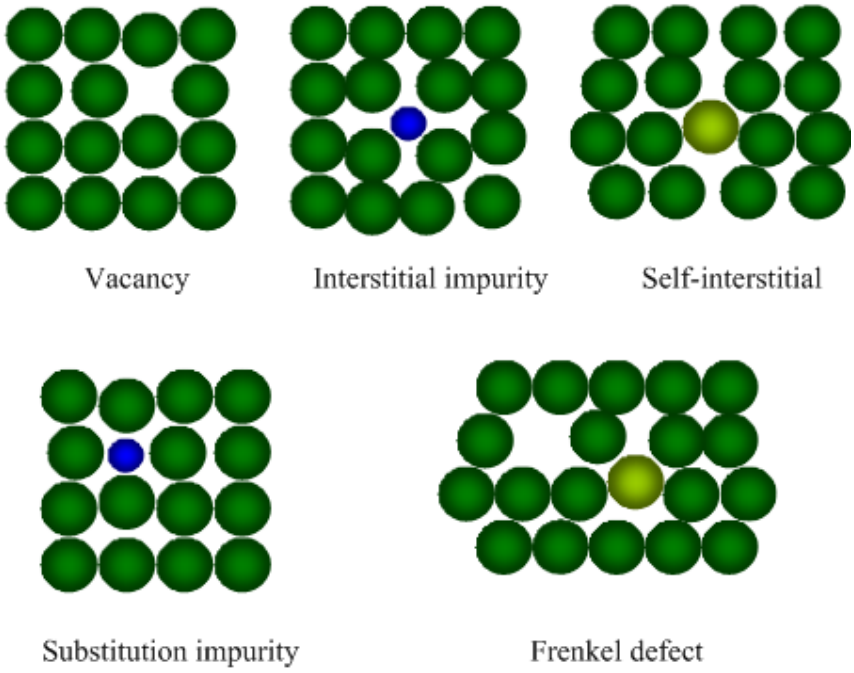

Fig 1.20 Various point defects in crystals

- Vacancy defects are lattice sites which would be occupied in a perfect crystal, but are vacant. If a neighboring atom moves to occupy the vacant site, the vacancy moves in the opposite direction to the site which used to be occupied by the moving atom. The stability of the surrounding crystal structure guarantees that the neighboring atoms will not simply collapse around the vacancy. In some materials, neighboring atoms actually move away from a vacancy, because they experience attraction from atoms in the surroundings. A vacancy is sometimes called a Schottky defect.
- Interstitial defects are atoms that occupy a site in the crystal structure at which there is usually not an atom. They are generally high energy configurations.
- A nearby pair of a vacancy and an interstitial is often called a Frenkel defect or Frenkel pair. This is caused when an ion moves into an interstitial site and creates a vacancy.

1.9.3.1 Schottky Defect

A Schottky defect is a type of point defect in a crystal lattice and is shown in Figure 1.21. The defect forms when oppositely charged ions leave their lattice sites, creating vacancies. These vacancies are formed in stoichiometric units, to maintain an overall neutral charge in the ionic solid.

(a) (b)

Figure 1.21 (a) Perfect crystal **(b)**Schottky defect

The vacancies are then free to move about as their own entities. Normally these defects will lead to a decrease in the density of the crystal. If in an ionic crystal of type, A+B- an equal number of cations and anions are missing from their lattice sites so that electrical neutrality as well as stoichiometry is maintained this is called a Schottky Defect. It is a vacancy defect and also a stoichiometric defect, as the ratio of the number of cations and anions remains the same and the arrangement is given in Figure 1.22. This type of defect is shown in compounds with highly ionic compounds and small difference in sizes of cations and anions.

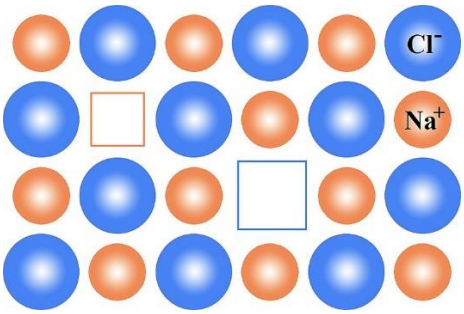

Fig 1.22 Arrangement of atoms in Schottky defect

1.9.3.2 Frenkel Defect

It is a type of point defect in a crystal lattice. The defect forms when an atom or cation leaves its place in the lattice, creating a vacancy, and becomes an interstitial by lodging in a nearby location not usually occupied by an atom and the arrangement is shown in Figure 1.23. Frenkel defects occur due to thermal vibrations. The Frenkel Defect is shown by ionic solids. The smaller ion is displaced from its lattice position to an interstitial site. It creates a vacancy defect at its original site and an interstitial defect at its new location. This defect does not change the density of the solid as it involves only the migration of the ions within the crystal.

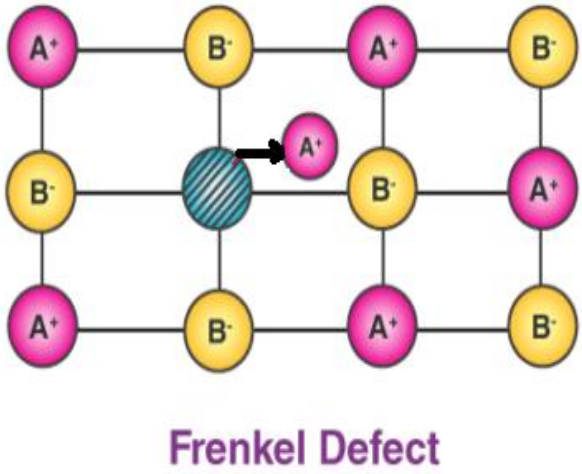

Fig 1.23 Arrangements of atoms in Frenkel defect.

1.10 Doping In ZnO

Doping intentionally introduces impurities into an extremely pure semiconductor for the purpose of modulating its electrical properties. The impurities are dependent upon the type of semiconductor. Doping a semiconductor is limited by local bonding effects, change in chemical potentials due to the presence of impurity atoms and the fermi-level induced compensation effects. ZnO is normally n-type due to defects and exhibits carrier concentration raging from 1016 cm-3 for high quality single crystals 41 cm-3 to 1021 cm-3 for intentionally doped samples. ZnO has strong applications in optoelectronic devices. In ZnO both n type and p type doping are possible. However, there is a difficulty in bipolar doping (i.e. both n and p types). Unipolar

doping has been seen in wide bandgap semiconductors such as ZnO, GaN, ZnS and ZnSe. With wide band gap ZnO can be easily doped ton type, while p type doping is difficult. The situation is opposite for ZnTe where p type doping is easily obtained, while n type doping is difficult

1.10.1 n Type Doping

ZnO having wurtzite structure is usually a n-type semiconductor due to the presence of intrinsic defects such as O vacancies and Zn interstitials and is given in the Figure 1.24.

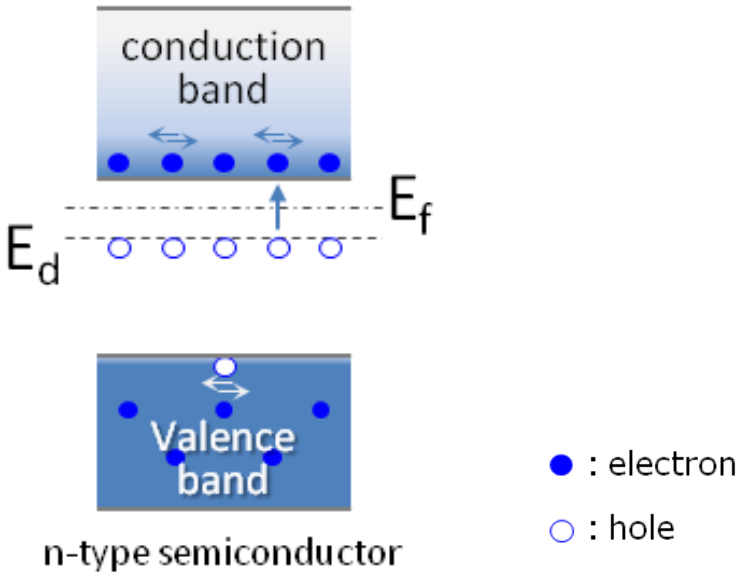

Figure 1.24 n type semiconductor

Although it is experimentally known that the doped ZnO is n type semiconductor whether the donors are Zinc interstitial or due to oxygen vacancy is still controversial. It is suggested that the n type ZnO is achieved due to the presence of hydrogen which acts as a shallow donor with ionization energy above 30 MeV (Van de Walle 2001; Strzhemechny *et al.* 2004). Ntype doping of ZnO is relatively easy compared to p type doping. Thus, n type doping is developed well. These are used in variety of applications as n type layers in light emitting diodes and transparent ohmic contacts

1.10.2 p Type Doping

It is very difficult to obtain p type doping in wide band gap semiconductors. The difficulties arises due to various reasons such as the dopants may be compensated by the low energy native

defects such as Zinc interstitials or oxygen vacancies and then due to the low solubility of the dopant and is given in Figure 1.25. Deep impurity level can also be a source of doping difficulty causing significant resistance to the formation of shallow acceptor level. It is suggested that the elements of group V are found to achieve p type doping though there are some difficulties (Park *et al.* 2002).

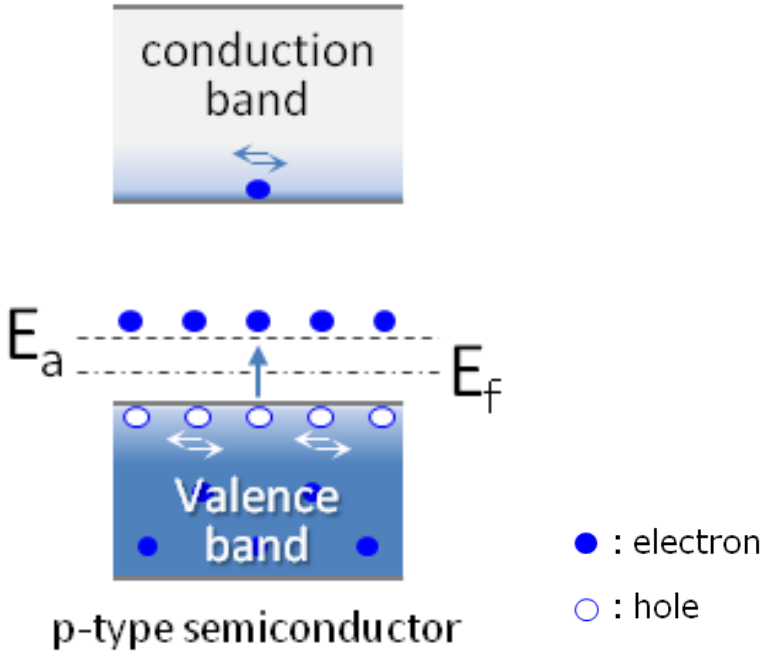

Figure 1.25 p type semiconductor

Also, p type doping in ZnO is possible with group I elements (Li, Na, K) for zinc sites or group V elements for oxygen sites. However, group I elements tend to occupy interstitial positions due to their smaller atomic radii rather than substitution (Look *et al.* 2004). Other p type doping possible in ZnO are Nitrogen doping (Iwata *et al.* 2000).

1.11 Basic physical properties of ZnO

Table 1 shows a compilation of the basic physical parameters of ZnO. Still some uncertainty exists in these values. For example, in few reports it has been mentioned physical properties of only p-type ZnO and therefore the hole mobility and effective mass are still in debates [22, 23]

Property	Value
Lattice parameter at 300 K	
A	3.2495 Å
C	5.2069 Å
c/a	1.602
Density	5.606 g cm-3
Stable phase at 300 K	Wurtzite
Bond length	1.977 μm
Melting point	1975°C
Thermal conductivity	0.6, 1-1.2
Static dielectric constant	8.656
Refractive index	2.008, 2.029
Energy gap	3.4 eV
direct Exciton binding energy	60 MeV
Iconicity	62%
Heat capacity Cp	9.6cal/mol K
Youngs modulus E (Bulk ZnO)	111.2 ± 4.7 Gp

Table 1 Basic physical properties of ZnO

1.11.1 Optical Properties of ZnO

The optical properties of a semiconductor are associated with both intrinsic and extrinsic effects. Intrinsic optical transitions take place between the electrons in the conduction band and holes in the valence band, including exitonic effects due to the Coulomb interaction. The main condition for exciton formation is that the group velocity of the electron and hole is equal. Excitons are classified into free and bound excitons. In high quality samples with low impurity concentrations, the free exciton can also exhibit excited states, in addition to their ground-state transitions. Extrinsic properties are related to dopants or defects, which usually create discrete electronic states in the band gap, and therefore influence both optical absorption and emission

processes. As we mentioned above, that ZnO is a direct band semiconductor and a transparent conductive material. ZnO films are transparent in the wavelength range of 0.3 and 2.5 μm, and plasma edge lies between 2 and 4 μm depending on the carrier concentration. It is well known that a shift in the band gap edge appears with an increase in the carrier concentration. This shift is known as Burstein-Moss shift. Optical transitions in ZnO have been studied by a variety of experimental techniques such as optical absorption, transmission, reflection, spectroscopic. ellipsometry, photoluminescence, cathodoluminescence, calorimetric spectroscopy, etc. Room temperature PL spectrum of ZnO is usually composed of a near UV-emission band (375 nm) and a green emission band (510 nm) although a yellow-orange band (610 nm) can also be observed in some situations. The near UV-band is closely related to the excitonic nature of the material and may be superposed with the free exciton emission, its phonon replica, bound exciton emission, as well as bi exciton emission. The observation of luminescence from exciton is usually difficult even at low temperatures. This comes from a lot of factors [21]: First, the efficiency of radiative emission is low even for direct gap semiconductors which are found to be 10-1 to 10-3. A large part of the radiative emission comes from bound-exciton complexes and defect centers. Secondly, exciton emission is limited by the internal reflection of the exciton and the small escape length. As a quasi-particle, exciton moves with their group velocity through the semiconductor. During its movement, exciton can be trapped or scattered by impurities and phonons. When it eventually reaches the surface of the semiconductor, in most cases, it will be reflected back into the semiconductor. Except the internal reflection, the radiative combination yield from free-exciton is also limited by the small escape length, which is defined as the depth from which exciton can reach the surface. Only the free-exciton inside the escape length can have the contribution to the luminescence. The research interest for the green band emission in ZnO can be traced back to the early stage of last century. Due to this green emission, ZnO is considered as an important luminescent material for the planar display and short-decay cathodoluminescence screens. Unfortunately, the mechanisms behind this emission band are still unclear even though the researches on this topic have been lasted for many years. Green band emission was first attributed to an excess of zinc. Almost all the proposed mechanisms about the green emission are attributed to the native lattice defects except the one that is based on the divalent Cu impurities[24].

1.11.2 Thermal Properties of ZnO

Thermal expansion coefficient (TEC)

The change in temperature affects the lattice parameters of semiconductors. Thermal expansion coefficients are defined as αa and αc for in and out of plane cases, respectively. The stoichiometry, presence of extended defects and free carrier concentration also affect the thermal expansion coefficient [25]

Thermal conductivity

Thermal conductivity (k), having a kinetic nature, is determined by vibration, rotation and electronic degree of freedom. It is really important property of semiconductors when these materials are used in high-power, high-temperature optoelectronic devices. The electronic thermal conductivity is very small, having light carrier concentration, which is negligible. For high pure crystals, phonon-phonon scattering is ideally proportional toT-1 at the temperatures higher than the Debye temperature. Point defects, such as vacancies, impurities and isotope fluctuations in ZnO affect the thermal conductivity of ZnO material [26].

1.11.3 Electrical Properties

As a direct and wide band gap semiconductor with a large exciton binding energy (60MeV), ZnO is representing a lot of attraction for optoelectronic and electronic devices. For example, a device made by material with a larger band gap may have a high breakdown voltage, lower noise generation and can operate at higher temperatures with high power operation. The performance of electron transport in semiconductor is different at low and high electric field. At sufficient low electric fields, the energy distribution of electrons in ZnO is unaffected much, because the electrons can't get much energy from the applied electrical field, as compared with their thermal energy. So the electron mobility will be constant because the scattering rate, which determines the electron mobility, doesn't change much. When the electrical field is increased, the energy of the electrons from the applied electrical field is equivalent to the thermal energy of the electron. The electron distribution function changes significantly from its equilibrium value. These electrons become hot electrons, whose temperature is higher than the lattice temperature. So

there is no energy loss to the lattice during a short and critical time. When the electron drift velocity is higher than its steady state value, it is possible to make a higher frequency device.

1.11.4 Chemical Properties

ZnO occurs as white powder commonly known as zinc white or as the mineral zincite. The mineral usually contains a certain amount of manganese and other elements and is of yellow to red color. Crystalline zinc oxide is thermo-chromic, changing from white to yellow when heated and in air reverting to white on cooling. This is caused by a very small loss of oxygen at high temperatures to form the non-stoichiometric Zn1+xO, where at 800 °C, x= 0.00007. Zinc oxide is an amphoteric oxide. It is nearly insoluble in water and alcohol, but it is soluble in (degraded by) most acids, such as hydrochloric acid:

$$ZnO + 2\ HCl \rightarrow ZnCl2 + H2O$$

Bases also degrade the solid to give soluble zincates:

$$ZnO + 2NaOH + H2O \rightarrow Na2(Zn(OH)4)$$

ZnO reacts slowly with fatty acids in oils to produce the corresponding carboxylates, such as oleate or stearate. ZnO forms cement-like products when mixed with a strong aqueous solution of zinc chloride and these are best described as zinc hydroxy chlorides. This cement was used in dentistry. ZnO also forms cement-like products when reacted with phosphoric acid, and this forms the basis of zinc phosphate cements used in dentistry. A major component of zinc phosphate cement produced by this reaction is hopeite, Zn3(PO4)2·4H2O. ZnO decomposes into zinc vapor and oxygen only at around 1975 °C, reflecting its considerable stability. Heating with carbon converts the oxide into zinc vapor:

$$ZnO + C \rightarrow Zn + CO$$

Zinc oxide reacts violently with aluminum and magnesium powders, with chlorinated rubber and linseed oil on heating causing fire and explosion hazard. It reacts with hydrogen sulfide to give the zinc sulfide: this reaction is used commercially in removing H2S using ZnO powder (e.g., as deodorant).

$$ZnO + H2S \rightarrow ZnS + H2O$$

When ointments containing ZnO and water are melted and exposed to ultraviolet light, hydrogen peroxide is produced.

1.12 Applications

ZnO has different chemical and physical properties. It can be used in numerous fields. Zinc oxide is important in a wide range of applications, from medicine to agriculture, from paints to chemicals and from tires to ceramics

1.12.1 Agricultural Applications

ZnO NPs have potential to enhance the growth of food crops. Seeds fixed by various ZnO NP concentrations improved seed propagation, seed strength and plant growth. ZnO NPs showed to be active in growing roots stems and seeds . Importance of zinc oxide NPs in biotechnology area was investigated by Paul and Ban . They observed the effect of chemically prepared ZnO NPs on the biological system. Zinc oxide is also used at different concentrations from (Streptococcus pneumonia, Bacillus subtitles, E.Coli and Pseudomonas aeruginosa). A quick rise of enzymatic activity was found through high concentrations of zinc oxide [27].

1.12.2 Medicinal Applications

Zinc oxide NPs have certain properties that make them appropriate for applications associated with the central nervous system (CNS) and possibly wit the improvement procedures of disease treatment over (mediating neuronal excitability) or (even the release of neurotransmitters). Several types of research have shown that zinc oxide influenced unalike tissues, cells or functions, as well as neural tissue engineering and biocompatibility [28].

1.12.3 The Pharmaceutical and Cosmetic Industries

Due to its antibacterial, disinfecting and drying properties, zinc oxide is widely used in the production of various kinds of medicines. It was formerly used as an orally administered medicine for epilepsy, and later for diarrhoea. At the present time it is applied locally, usually in the form of ointments and creams, and more rarely in the form of dusting powders and liquid powders. ZnO has properties which accelerate wound healing, and so it is used in dermatological substances against inflammation and itching. In higher concentrations it has a peeling effect. It is

also used in suppositories. In addition it is used in dentistry, chiefly as a component of dental pastes, and also for temporary fillings. ZnO is also used in various types of nutritional products and diet supplements, where it serves to provide essential dietary zinc . For many years, before sun creams began to contain nanoparticles of ZnO or TiO2, they contained thick preparations which did not rub easily into the skin and which were cosmetically unattractive. Due to their ability to absorb UVA and UVB radiation, these products began to be used in creams. A new cream formula, containing a combination of ZnO and TiO2, solved the problem of an insufficiently white layer and produced a new medium which is more transparent, less adhesive and much more easily rubbed into the skin . A number of studies have shown that titanium and zinc oxides are extremely good media in sun creams, since they absorb UV radiation, do not irritate the skin, and are easily absorbed into the skin .

1.12.4 The Textile Industry

onto a fibrous substrate by a low-temperature growth technique provided excellent UV protection. The textile industry offers a vast potential for the commercialization of nanotechnological products. In particular, water repellent and self-cleaning textiles are very promising for military applications, where there is a lack of time for laundering in severe conditions. Also in the world of business, self-cleaning and water repellent textiles are very helpful for preventing unwelcome stains on clothes. Protection of the body from the harmful UV portion of sunlight is another important area. Many scientists have been working on selfcleaning, water repellent and UV-blocking textiles. For textile applications, not only is zinc oxide biologically compatible, but also nano structured ZnO coatings are more air-permeable and efficient as UV-blockers compared with their bulk counterparts. Therefore, ZnO nanostructures have become very attractive as UV-protective textile coatings. Different methods have been reported for the production of UV-protecting textiles utilizing ZnO nanostructures. For instance, hydrothermally grown ZnO nanoparticles in SiO2-coated cotton fabric showed excellent UV-blocking properties. Synthesis of ZnO nanoparticles elsewhere through a homogeneous phase reaction at high temperatures followed by their deposition on cotton and wool fabrics resulted in significant improvement in UVabsorbing activity. Similarly, ZnO-nanorod arrays that were grown

1.12.5 The Electronics and Electro technology Industries

Zinc oxide is a new and important semiconductor which has a range of applications in electronics and electro technology. Its wide energy band (3.37 eV) and high bond energy (60 meV) at room temperature mean that zinc oxide can be used in photo electronic and electronic equipment , in devices emitting a surface acoustic wave , in field emitters , in sensors , in UV lasers , and in solar cells . ZnO also exhibits the phenomenon of luminescence (chiefly photoluminescence emission of light under exposure to electromagnetic radiation). Because of this property it is used in FED (field emission display) equipment, such as televisions. It is superior to the conventional materials, sulfur and phosphorus (compounds exhibiting phosphorescence), because it is more resistant to UV rays, and also has higher electrical conductivity. The photoluminescent properties of zinc oxide depend on the size of crystals of the compound, defects in the crystalline structure, and also on temperature. ZnO is a semiconductor, and thin films made of that material display high conductivity and excellent permeability by visible rays. These properties mean that it can be used for the production of light-permeable electrodes in solar batteries. It also has potential uses as a transparent electrode in photovoltaic and electroluminescent equipment, and is a promising material for UV-emitting devices. Zinc oxide is also used in gas sensors. It is a stable material whose weak selectivity with respect to particular gases can be improved by adding other elements. The working temperature of ZnO is relatively high (400–500 °C), but when nanometric particles are used this can be reduced to around 300 °C. The sensitivity of such devices depends on the porosity and grain size of the material; sensitivity increases as the size of zinc oxide particles decreases. It is most commonly used to detect CO and CO2 (in mines and in alarm equipment), but can also be used for the detection of other gases (H2, SF6, C4H10, C2H5OH). The zinc oxide used in the production of such equipment is obtained by a variety of methods (chemical vapour deposition, aerosol pyrolysis or oxidation of metallic zinc); it is important to control the process temperature, since this determines the properties of the product. One of the most important applications of zinc oxide in electronics is in the production of varistors. These are resistors with a non-linear current-voltage characteristic, where current density increases Materials rapidly when the electrical field reaches a particular defined value. They are used, among other things, as lightning protectors, to protect high-voltage lines, and in electrical equipment providing protection against atmospheric and network voltage surges. These applications require a material of high

compactness, since only such a material can guarantee the stability and repeatability of the characteristics of elements made from it .

1.12.6 Photocatalysis

Intensive scientific work has taken place in recent years on photocatalysis. In this process, an electron-hole pair is produced below the intensity of light by means of oxidation or reduction reactions taking place on the surface of the catalyst. In the presence of a photocatalyst, an organic pollutant can be oxidized directly by means of a photogenerated hole or indirectly via a reaction with characteristic reactive groups (ROS), for example the hydroxyl radical OH·, produced in solution. The most commonly used catalysts are TiO2 and ZnO. TiO2 exhibits photocatalytic activity below the intensity of UV light. ZnO provides similar or superior activity to that of TiO2, but is less stable and less sensitive to photocorrosion. Better stability, however, is provided by zinc oxide of nanometric dimensions, which offers better crystallinity 26 and smaller defects. The photocatalytic activity of ZnO can be further improved, and the range of the visible spectrum for zinc oxide can be extended, by adding other components [29].

LITERATURE REVIEW

Bing-Chang Jiang *et al.* reports the growth of 3 mol% nickel (Ni)-doped zinc oxide nanowalls(ZnO NWLs) with Enhanced Electron Transport Ability for Electrochemical Water Splitting using the hydrothermal method and they characterized prepared sample using SEM ,AFM,XRD,FTIR and EDAX. Compared with the undoped ZnO, Ni-doped ZnO NWLs have more staggered networks, indicative of greater surface area. Both the undoped and Ni-doped ZnO NWLs showed sponge-like nanostructures through SEM observation. Moreover, the pores of Ni-doped.ZnO NWLs are obviously smaller and uniform than the undoped one. Morphological investigation as well as electrical conductivity of the undoped and Ni-doped ZnO NWLs was also discussed. The surface roughnessof the formed ZnO NWLs was reduced after Ni-doping.The electrical conductivity of the electron-only device based on the Ni-doped ZnO NWLs was higher than that of the undoped one. XRD pattern reveals that the polycrystalline of

hexagonal wurtzite structure and the average size of the particles were estimated. The FTIR result shows the stretching vibration of the Zn-O bond in Ni doped ZnO nanoparticles [30].

Mohammad Ruhul Amin Bhuiyan *et al.* studied the key ideas and themes of the possibility of growing Ni doped ZnO nanoparticles by electrochemical method. And they characterized prepared sample using various techniques such as XRD, SEM, FTIR, photoluminescence spectroscopy together with the measured optical parameters obtained from UV-VIS absorption testing were analyzed . The purpose is to study the growth mechanism and to optimize the parameters of this method. XRD pattern reveals that the polycrystalline of hexagonal wurtzite structure and the average size of the particles were estimated to be approximately 61 nm, which conform the nanoparticle. The FTIR result shows the stretching vibration of the Zn-O bond in Ni doped ZnO nanoparticles. There is a green emission peak centered at about 384 nm in the PL behavior. The band edge is shifted to the lower energy side of the Ni doped ZnO nanoparticle. Analyzing the results of various types of characterizations, it has been assessed that Ni doped ZnO nanoparticles was successfully synthesized [31].

Pallavi G.Undre *et al.* conducted a systematic investigations on the structural, morphological and electrical properties of $Zn_{1-x}Ni_xO$ (x = 0.00, 0.03 and 0.05) nanoparticles synthesized via sol-gel auto combustion technique and the prepared samples were characterized by X-ray diffraction technique (XRD) and scanning electron microscopy (SEM). X-ray diffraction pattern shows the formation of single phase with hexagonal wurtzite structure. The lattice parameter of Ni doped ZnO is slightly greater than that of un-doped ZnO nanoparticles. The crystalline size of prepared nanoparticles is found to be in 30 to 32 nm. SEM image shows that the grains are in nanometre range which confirms the nanocrystalline nature of present samples. The temperature dependent DC electrical resistivity measurements have been carried out in the temperature range of 303-573K. The DC electrical resistivity was found to increase with increase in Ni^{2+} concentration into ZnO matrix. The resistivity decreases with increasing temperature which interpreted semiconducting nature of ZnO nanoparticles [32].

C. Soumya *et al*. synthesized Nickel doped zinc oxide ($Zn_{1-x}O$, x=0wt%, 1 wt%, 2wt %) via solid state reaction method and the structural and optical characterizations were carried out with

the prepared samples. Structural characteristics were determined by X- ray diffraction method, Raman spectroscopic analysis. Optical property studies of the sample were done through the UV-VIS- spectral analysis. The structural studies confirmed the hexagonal wurtzite structure of zinc oxide and the spectroscopic analysis shows a decrease in optical band gap from 3.37eV to 2.9eV [33].

Neelakanta Reddy *et al.* prepared Ni-doped ZnO samples at various Ni molar concentrations via a simple solid state reaction and the phase analysis, surface morphology, chemical structure, and optical properties of the pure and doped ZnO were investigated using a PANalytical X-ray diffractometer (XRD), scanning electron microscope (SEM, Hitachi S-4800, Japan), high-resolution transmission electron microscope (HR-TEM, G2 F30 S-Twin), X-ray photoelectron spectroscope (XPS, Thermo Fisher Scientific MultiLab 2000), Raman spectrometer (XploRA Plus: 532 nm), and a Horiba photoluminescence spectrometer. The formation of Ni-doped ZnO were confirmed by various analysis techniques. 1 mol% Ni-doped ZnO structures showed the maximum photoelectrochemical activity under visible light. The maximum current density of ~3.28 mA cm^{-2} in a 0.1 M NaOH electrolyte demonstrated a superior charge separation. The photocurrent density of 1 mol% Ni-doped ZnO structures showed 12 times maximum currents than that of pristine ZnO under visible light illumination. Ni-doping into ZnO sites increases efficient electron-hole separation and transfer, significantly reduces the rate of recombination. The obtained data are anticipated to be considerably supportive in evolving cheap, modest synthesis approaches and enhanced photoelectrodes for photoelectrochemical applications [34].

K. Nomita Devi *et al.* synthesized Nickel doped zinc oxide $Zn_{1-x}Ni_xO$ ($x = 0$, 0.02, 0.04, 0.06, 0.08, 0.1) with improved photocatalytic activity for Malachite Green Dye degradation and parameters affecting the degradation using chemical co-precipitation method and the structural, morphological and optical properties of the synthesized samples were investigated using XRD (X-ray diffraction), SEM (scanning electron microscope), EDX (energy-dispersive X-ray), TEM (transmission electron microscope), FTIR (Fourier transform infrared) and UV–Vis spectroscopy. The photocatalytic activities of the synthesized samples toward the degradation of Malachite Green (MG) dye under UV light irradiation were studied. $Zn_{0.94}Ni_{0.06}O$ was observed to be the better photocatalyst among the studied samples which degrades 77% of the dye under 4 h of irradiation. The effect of operational parameters such as catalyst dosage, initial dye

concentration and pH on the degradation percentage was investigated. An optimum condition was obtained for a catalyst load of 0.10 g/L into 15 ppm dye solution at pH 9 which degrades 76% of the dye under 1hour of UV irradiation. Reusability test of the photocatalyst was also performed to check the stability for long-term application of the samples [35].

Navendu Goswami *et al*. synthesized ZnO nanostructures with 1-10% of Ni doping adopting a chemical precipitation method and the prepared undoped and doped nanostructures were characterized by X-ray diffraction (XRD), transmission and scanning electron microscopy (TEM/SEM), Fourier transform infrared (FTIR) and micro-Raman spectroscopy (μRS). The identification of wurtzite phase and determination of lattice parameters of Ni doped ZnO nano crystallites is ascertained through XRD analysis. TEM/SEM images reveal the structural alteration of ZnO with variation of Ni doping concentrations. The study of vibrational modes of nanostructures at different stages of structural transformation, as performed through FTIR and Raman spectroscopy, assist in deciphering the crucial role of Ni doping concentration in gradual evolution of nickel doped ZnO structure from nanoparticles to nanorods [36].

Wolska-Kornio *et al.* (2016) has developed europium doped ZnO nano powders via microwave hydrothermal method. The structural, morphological and optical properties was investigated by synthesized europium doped ZnO nanomaterials [37].

Kumari et al., (2015) studied influence of nitrogen doping on structural and optical properties of ZnO nano particles. Undoped and N doped ZnO nano particles were synthesized by using chemical precipitation method. The prepared samples were differentiated through X-Ray Diffraction technique (XRD), Transmission Electron Microscopy (TEM) equipped with Energy Dispersive X-ray (EDAX) spectroscopy, UV–visible spectroscopy, Fourier Transform Infrared(FTIR) and came to a conclusion that the formation of impurity free wurtzite phase for undoped and N doped samples was uncertain through XRD analysis. The crystallite size was found increasing with increase in N doping concentration [38].

Mohan, et al.,(2016) conducted a study on the preparation of zinc oxide nanoparticles using conventional process and the preparation using surfactant and with characterization of the prepared zinc oxide using Scanning Electron Microscopy (SEM) and X-Ray Diffraction in order

to find out which method is more feasible in terms of particle agglomeration, particle size, particle separation**.** They stated that zinc oxide nanoparticles were successfully prepared with and without using surfactants. The characterization results it's clear that the conventional method of preparation highly affected by particle agglomeration and also the particle separation is not good enough. And the most important thing is that the particle size of zinc oxide prepared using PVA is in the nano meter's range whereas in conventional method of preparation particle size in the micron range [39].

J.N.Hasnidawani *et al.*(2016) synthesized ZnO nanoparticles via sol gel method using Zinc acetate dehydrate ($Zn(CH_3COO)_2.2H_2O$) as a precursor and ethanol (CH_2COOH) was used as solvent, Sodium hydroxide (NaOH) and distilled water were used as medium. ZnO nanoparticles were characterized by using XRD, EDX, FESEM, and nano-particles analyser. Result of EDX characterization shows that the ZnO nanoparticles has good purity with (Zinc content of- 55.38% and; Oxygen content of- 44.62%). XRD result spectrum displays mainly oxygen and zinc peaks, which indicate the crystallinity in nature as exhibited. FESEM micrographs shows that synthesized ZnO have a rod-like structure. The obtained ZnO nanoparticles are homogenous and consistent in size which corresponds to the XRD result that exhibit good crystallinity. ZnO nanoparticles were successfully synthesized by sol-gel method in nanosize range within 81.28 nm to 84.98 nm [40].

Kenneth Maduabuchi Ezealisiji *et al*,(2019) synthesized zinc oxide nanoparticles (ZnO NPs) prepared via a precipitation method. Green synthesized ZnO NPs have a wide range of uses such as biomedical applications, water purification, optical devices and gas sensors. The non-toxic and economical technique described in this article is favorable for large-scale production too. ZnO NPs were produced from a zinc acetate precursor with dye extract of Ixora Coccinea (IC) leaves as a capping agent. The as-prepared ZnO NPs were characterized by X-ray diffraction (XRD), Fourier transform infrared (FTIR), UV-visible (UV-vis), scanning electron microscopy (SEM) and energy dispersive X-ray (EDX) techniques. The XRD analysis showed an average crystallite size of 23 nm. The SEM analysis revealed a reduction in aggregation of ZnO crystallites due to addition of dye extracts of IC. EDX and UV-vis results confirmed the formation of pure ZnO NPs [41].

Robina Ashraf *et al*, (2013) ZnO nanoparticles with particle size less than 50nm by simple solgel method. These nanoparticles can be used as a source layer for the extraction of electrons in heterojunction organic solar cells. Zinc acetate is used as a precursor material in this case. X-Ray powder Diffraction, Ellipsometry and Scanning Electron Microscopy are used to study the crystal structure, optical properties and surface morphology of the synthesized nanoparticles, respectively. The presence of (100),(002) and (101) planes in the XRD graphs strongly indicates that ZnO has wurtzite structure even under as-synthesized conditions. Surface morphology was studied by SEM which indicates that the nanoparticles are of spherical shape with size less than100 nm. Large area growth of these nanoparticles is also observed with uniform size distribution [42].

Ehsan Zaman *et al*,(2015) were successfully produced ZnO-Al2O3 mixed oxide nanoparticles from a solution containing Zn (acetate) and AlCl3 by Solvothermal method. The calcination process of the ZnO-Al2O3 composite nanoparticles brought forth polycrystalline two-phaseZnO-Al2O3 nanoparticles of 30 – 50 nm in diameters. ZnO and Al2O3 were crystallized into wurtzite and rock salt structures, respectively. The optical properties of ZnO-Al2O3 nanoparticles were determined with solid state UV and florescent (PL). The structure properties of this sample were analysed by XRD, SEM and Raman spectroscopy and then comparison with baulk case of these samples [43].

Carmen Mihaela Topala *et al*,(2019) synthesized Undoped and Al-doped ZnO (AZO) powders by hydrolytic and hydrothermal synthesis from Zn(NO3)2 , AlCl3 using KOH 1M concentration like hydrolysis agent. The structural properties of prepared powders were studied using XRD and FTIR spectroscopy. Presence of aluminium in the hydrothermal powders is correlated with the presence of Zn-Al hydrotalcite like structure [44].

References

[1] A. Dowling, et al., Nanoscience and nanotechnologies: opportunities and uncertainties, A Report by The Royal Society & The Royal Academy of Engineering, London, July 2004.

[2] C. P. Poole, Jr., F. J. Owens, Introduction to Nanotechnology, Wiley-Interscience, Hoboken, NJ, 2003.

[3] C. M. Lieber, MRS Bull. 2003, 28, 486.

[4] Journal of Nanoscience and Nanoengineering Vol. 1, No. 4, 2015, pp. 248-251

[5] Handbook on Nanoscience, Engineering and Technology, 2nd ed., Taylor and Francis, 2007, pages 3.1-3.26.

[6] Introduction to Nanotechnology, by Charles P. Poole Jr. and Frank J. Owens. ISBN 0-471-07935-9. Copyright Q 2003 John Wiley & Sons, Inc.

[7] JE Hulla, SC Sahu, AW Hayes - Human & experimental …, 2015 - journals.sagepub.com

[8] Hochella, M. F., Jr.; Spencer, M. G.; Jones, K. L. Environ. Sci.: Nano 20. 2015, 2, 114–119. doi:10.1039/C4EN00145A

[9] 20. Sharma, V. K.; Filip, J.; Zboril, R.; Varma, R. S. Chem. Soc. Rev. 22. 2015, 44, 8410–8423. doi:10.1039/C5CS00236Bv

[10] Wagner, S.; Gondikas, A.; Neubauer, E.; Hofmann, T.; von der Kammer, F. Angew. Chem., Int. Ed. 2014, 53, 12398–12419. doi:10.1002/anie.201405050

[11] NANOMATERIALS By:Dr. R. K. Mohapatra, M.Sc., M.Phil., M.B.A., Ph.D. Faculty (Chemistry), GCE Keonjhar

[12] Recent Advances on Classification, Properties, Synthesis, and Characterization of Nanomaterials by Veer Singh, Priyanka Yadav, and Vishal Mishra School of Biochemical Engineering, IIT (BHU), Varanasi, Uttar Pradesh, India

[13] Kamigaito, O (1991). "What can be improved by nanometer composites?". J. Jpn. Soc. Powder Powder Metall. 38 (3): 315–21. doi:10.2497/jjspm.38.315. in Kelly, A, Concise encyclopedia of composites materials, Elsevier Science Ltd, 1994

[14] FABRICATION OF NANOMATERIALS BY TOP-DOWNAND BOTTOM-UP APPROACHES – AN OVERVIEW Dr. V.M.Arole1, Prof.S.V.Munde2 JAAST:Material Science (Special Issue) December – 2014 Vol. 1|Issue 2|Page 89-93

[15] Sciencedirect.com/topics/chemistry/ball milling

[16] en.wikipedia.org/wiki/Electron-beam-lithography

[17] tandfonline.com/doi/full/10.1080/23746149.2016.1142828

[18] hindawi.com/journals/amse/2021/5102014

[19] Sciencedirect.com/topic/materials-science/electrodeposition

[20] J. Geurts, Zinc Oxide: From Fundamental Properties Towards Novel Applications, By CF Klingshirn Al 120 (2010).

[21] Z. L. Wang, X. Y. Kong, Y. Ding, P. Gao, W. L. Hughes, R. Yang, Y. Zhang, Semiconducting and piezoelectric oxide nanostructures induced by polar surfaces, Adv. Funct. Mater. 14(10) (2004) 943–956

[22] Gunter Horst “The characterization of bulk as-grown and annealed ZnO by Hall effect” PhD thesis, University of Pretoria, Pretoria.

[23] W. Gopel, J. Pollmann, I. Ivanov and B. Reihl, Phys. Rev. B 26, 3144-3150 (1982).

[24] T. Olorunyolemi, A. Birnboim, Y. Carmel, O. C. Wilson, Jr and I. K. Lloyd, J. Am. Ceram. Soc. 85, 1249 (2002).

[25] D. C. Look, J. W. Hemsky, J. R. Sizelove, Phys. Rev. letters Vol. 82, No. 12 (1999).

[26] Chennupati Jagadish and Stephen J.Pearton “Zinc Oxide Bulk, Thin films and edition (2006).

[27] (Prasad J.el al Journal of plant nutrition 35(6) 2012

[28] Osmond M.J and Mccall MJ nanotoxicology

[29] Pauli s and Ban ,DK, international journal of advances in chemical engineering and biological sciences (IJACEBS),2014

[30] https://www.mdpi.com/2079-4991/11/8/1980

[31] https://www.researchgate.net/publication/262007128_Effect_of_nickel_doping_on physical_properties_of_zinc_oxide_thin_films_prepared_by_the_spray_pyrolysis_method

[32] https://www.sciencedirect.com/science/article/pii/S2452177917300506

[33] https://aip.scitation.org/doi/10.1063/5.0029876

[34] https://iopscience.iop.org/article/10.1088/2053-1591/ab0763

[35] https://link.springer.com/article/10.1007/s10854-021-05545-x

[36] https://www.cambridge.org/core/journals/mrs-online-proceedings-library-archive

[37] https://www.researchgate.net/publication/325398584 Tuning the luminescence of ZnOEu_nanoparticles_for_applications_in_biology_and_medicine

[38] Kumari, R., Sahai, A., & Goswami, N. (2015). Effect of nitrogen doping on structural and optical properties of ZnO nanoparticles. *Progress in Natural Science: Materials International*, *25*(4), 300-309.

[39] Mohan, A. C., & Renjanadevi, B. (2016). Preparation of zincoxide nanoparticles and its characterization using scanning electron microscopy (SEM) and X-ray diffraction (XRD). *Procedia Technology*, *24*, 761-766

[40] J.N. Hasnidawani , H.N. Azlina , H. Norita1, N.N. Bonnia, S. Ratim and E.S. Ali (2016). Synthesis of ZnO Nanostructures Using Sol-Gel Method. *Procedia Chemistry 19*, 211 – 216

[41] Kenneth Maduabuchi Ezealisiji, Xavier Siwe-Noundou, Blessing Maduelosi, Nkemakolam Nwachukwu, Rui Werner Maçedo Krause (2019). Green synthesis of zinc oxide nanoparticles using Solanum torvum (L) leaf extract and evaluation of the toxicological profile of the ZnO nanoparticles–hydrogel composite in Wistar albino rats. *International Nano Letters (2019)* 9:99–107

[42] Synthesis and Characterization of ZnO Nanoparticles (2013). Robina Ashraf, Saira Riaz, Muhammad Khaleeq-ur-Rehman and Shahzad Naseem. *The 2013 World Congress on Avances in nano,Bio mechanics, Robotics, and Energy Resarch*, Korea, Aug 23-28, 2013.

[43] Solvothermal Synthesis, Characterization and OpticalProperties of ZnO and ZnO-Al2O3 Mixed Oxide Nanoparticles. (2015) Ehsan Zamani, Fatemeh Rezaei, Sara Bagheri, Mahdieh Ghobadifard, Maryam Mahmoudi, Saeid Farhadi, Abedin Zebardasti and Alireza Aslani. Int. J. Nano. Chem.1, No. 1, 19-23 (2015).

[44] Carmen Mihaela Topala, Adriana Gabriela Plaiasu, Catalin Marian Ducu, Sorin Georgian Moga (2019) Structural Characterization of ZnO and Al Doped ZnOPowders Synthesis in Aqueous Solutions. *REV.CHIM.(Bucharest),70,No. 9,*2019

CHAPTER 2

CHARACTERIZATION TECHNIQUES

2.0 Introduction

Nanoscience and nanotechnology are considered to be the key technologies for the current century. The fundamental of nanotechnology lies in the fact that size is reduced to the nanometer range. But measuring this nano dimension is not a very easy task. Although research is going on to synthesize nanostructured and nanophasic materials, characterizing these nano sized materials is now an established field. Thus, nanotechnology has motivated the upsurge in research activities on the discovery and invention of sophisticated nano characterization technique to allow a better control of structural analysis, morphology, properties, size and dimensions of a materials in nano range [1].

2.1 Different Types of Characterization Technique

2.1.1 X-Ray Diffraction (XRD)

X-ray diffraction is a powerful tool for materials characterization. Typically, XRD provides information regarding the crystalline structure, nature of the phase, lattice parameters and crystalline grain size. The latter parameter is estimated by using the Scherrer equation using the broadening of the most intense peak of an XRD measurement for a specific sample. The Scherrer equation can be written as:

$$D = k\lambda/\beta cos\theta \quad \text{..... (1)}$$

Where:

K is a dimensionless shape factor with a value close to unity.

λ is the X-ray wavelength.

θ is the Bragg angle.

2.1.1.2 Principle

The materials are made of using atoms and those are systematically arranged into a crystal structure. When the X-ray beams are fall on the surface of a crystal plane (sample) with an angle called glancing angle (θ). The X-ray beams are reflected from the atomic plane, called as a diffracted beam. If the reflected X-ray wave undergoes constructive interference, they are said to be diffracted by the crystal plane [2]. The intensity of diffracted X-ray beam is the function of incident angle 2θ and it produces diffraction pattern [3].

$$n\lambda = 2d \sin\theta \quad \ldots\ldots\ldots\ldots\ldots\ldots\ldots\ldots\ldots\ldots \quad (2)$$

Where:

n = integer

λ = wavelength of X-ray radiation

d = spacing between the set of crystal planes

θ = glancing angle between the radiation and surfaces

The X-ray diffraction can be interpreted by Bragg's law and it can be understood by the following Fig 2.1

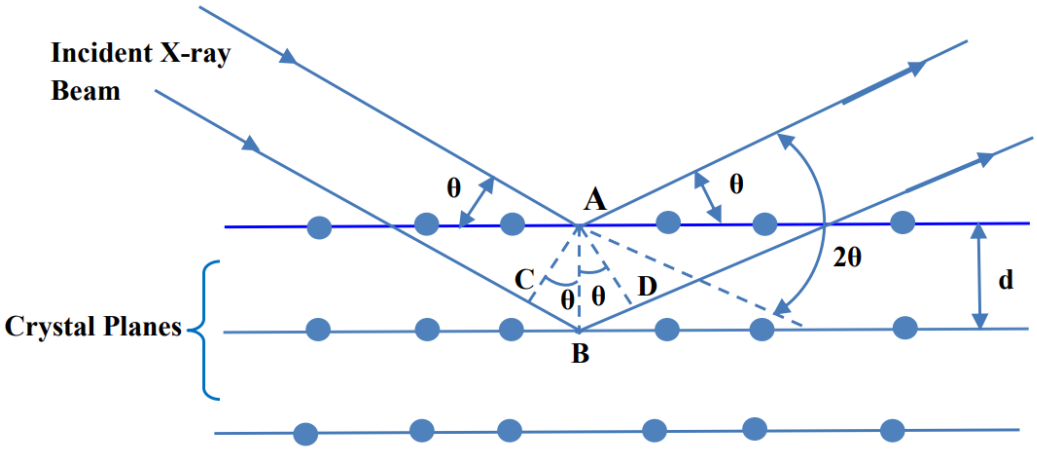

Figure 2.1 Diffraction of X-rays from the crystal plane.

In the above diagram the incident X-Rays have fixed values of wavelength and interplanar distance d is constant. The diffraction occurs at several angles of incidence such as θ1, θ2, θ3,.. corresponding to n = 1, 2, 3,… the order of reflection. If the difference between their path lengths is zero or an integer multiple of wavelength then these two waves are completely in phase and constructive interference pattern occurs. When the difference between the two rays is λ/2 then these two waves are out of phase and destructive interference pattern occurs [4]. The crystal structure of any substance scatters X-ray wavelength in its own unique diffraction pattern is also called as fingerprint of its atomic and molecular structure [2].

2.1.1.3 Instrumentation

X-ray diffractometers consist of three basic elements: an X-ray tube, a sample holder, and an X-ray detector.

Figure 2.2 Bruker's X-ray Diffraction

X-rays are generated in a cathode ray tube by heating a filament to produce electrons, accelerating the electrons toward a target by applying a voltage, and bombarding the target material with electrons. When electrons have sufficient energy to dislodge inner shell electrons

of the target material, characteristic X-ray spectra are produced. These spectra consist of several components, the most common being K_α and K_β. K_α consists, in part, of $K_{\alpha 1}$ and $K_{\alpha 2}$. $K_{\alpha 1}$ has a slightly shorter wavelength and twice the intensity as $K_{\alpha 2}$. The specific wavelengths are characteristic of the target material (Cu, Fe, Mo, Cr). Filtering, by foils or crystal monochromators, is required to produce monochromatic X-rays needed for diffraction. $K_{\alpha 1}$and $K_{\alpha 2}$ are sufficiently close in wavelength such that a weighted average of the two is used. Copper is the most common target material for single-crystal diffraction, with Cu K_α radiation = 1.5418Å. These X-rays are collimated and directed onto the sample. As the sample and detector are rotated, the intensity of the reflected X-rays is recorded. When the geometry of the incident X-rays impinging the sample satisfies the Bragg Equation, constructive interference occurs and a peak in intensity occurs. A detector records and processes this X-ray signal and converts the signal to a count rate which is then output to a device such as a printer or computer monitor.

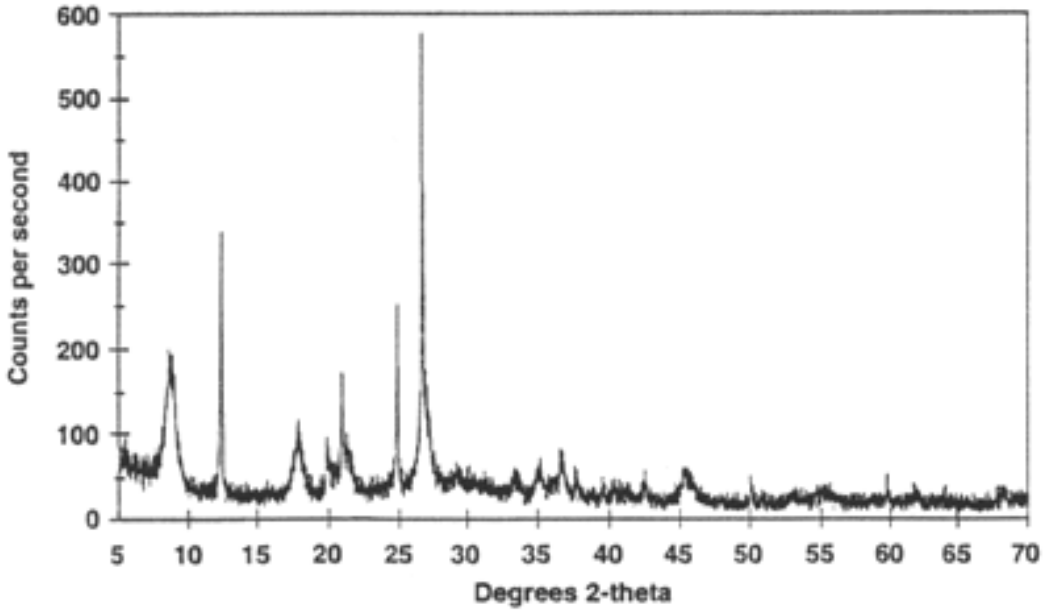

The geometry of an X-ray diffractometer is such that the sample rotates in the path of the collimated X-ray beam at an angle θ while the X-ray detector is mounted on an arm to collect the diffracted X-rays and rotates at an angle of 2θ. The instrument used to maintain the angle and rotate the sample is termed a *goniometer*. For typical powder patterns, data is collected at 2θ from ~5° to 70°, angles that are present in the X-ray scan [5].

2.1.1.4 Applications

- X-ray powder diffraction is most widely used for the identification of unknown crystalline materials (e.g. minerals, inorganic compounds).
- Determination of unknown solids is critical to studies in geology, environmental science, material science, engineering and biology.
- Characterization of crystalline materials
- Identification of fine-grained minerals such as clays and mixed layer clays that are difficult to determine optically
- Determination of unit cell dimensions
- Measurement of sample purity

2.1.1.5 Strengths

- Powerful and rapid (< 20 min) technique for identification of an unknown mineral
- In most cases, it provides an unambiguous mineral determination
- Minimal sample preparation is required
- XRD units are widely available

2.1.1.6 Limitations

- Homogeneous and single phase material is best for identification of an unknown
- Must have access to a standard reference file of inorganic compounds (d-spacings, hkls)
- Requires tenths of a gram of material which must be ground into a powder
- For mixed materials, detection limit is ~ 2% of sample [5].

2.1.2 Scanning Electron Microscope (SEM)

The scanning electron microscope (SEM) uses a focused beam of high-energy electrons to generate a variety of signals at the surface of solid specimens. The signals that derive

from electron-sample interactions reveal information about the sample including external morphology (texture), chemical composition, and crystalline structure and orientation of materials making up the sample. In most applications, data are collected over a selected area of the surface of the sample, and a 2-dimensional image is generated that displays spatial variations in these properties. Areas ranging from approximately 1 cm to 5 microns in width can be imaged in a scanning mode using conventional SEM techniques (magnification ranging from 20X to approximately 30,000X, spatial resolution of 50 to 100 nm). The SEM is also capable of performing analyses of selected point locations on the sample; this approach is especially useful in qualitatively or semi-quantitatively determining chemical compositions (using EDS), crystalline structure, and crystal orientations (using EBSD). The design and function of the SEM is very similar to the EPMA and considerable overlap in capabilities exists between the two instruments [6].

Figure 2.3 A typical SEM instrument,

2.1.2.1 Principle

Accelerated electrons in an SEM carry significant amounts of kinetic energy, and this energy is dissipated as a variety of signals produced by electron-sample interactions when the incident electrons are decelerated in the solid sample. These signals include secondary electrons (that produce SEM images), backscattered electrons (BSE), diffracted backscattered electrons (EBSD

that are used to determine crystal structures and orientations of minerals), photons (characteristic X-rays that are used for elemental analysis and continuum X-rays), visible light (cathodoluminescence-CL), and heat. Secondary electrons and backscattered electrons are commonly used for imaging samples: secondary electrons are most valuable for showing morphology and topography on samples and backscattered electrons are most valuable for illustrating contrasts in composition in multiphase samples (i.e., for rapid phase discrimination). X-ray generation is produced by inelastic collisions of the incident electrons with electrons in discrete ortitals (shells) of atoms in the sample. As the excited electrons return to lower energy states, they yield X-rays that are of a fixed wavelength (that is related to the difference in energy levels of electrons in different shells for a given element). Thus, characteristic X-rays are produced for each element in a mineral that is "excited" by the electron beam. SEM analysis is considered to be "non-destructive"; that is, x-rays generated by electron interactions do not lead to volume loss of the sample, so it is possible to analyze the same materials repeatedly [6].

2.1.2.2 Instrumentation

Essential components of all SEMs include the following:

- Electron Source ("Gun")
- Electron Lenses
- Sample Stage
- Detectors for all signals of interest
- Display / Data output devices
- Infrastructure Requirements:
    - Power Supply
    - Vacuum System
    - Cooling system
    - Vibration-free floor
    - Room free of ambient magnetic and electric fields

SEMs always have at least one detector (usually a secondary electron detector), and most have additional detectors. The specific capabilities of a particular instrument are critically dependent on which detectors it accommodates.

2.1.2.3 Working

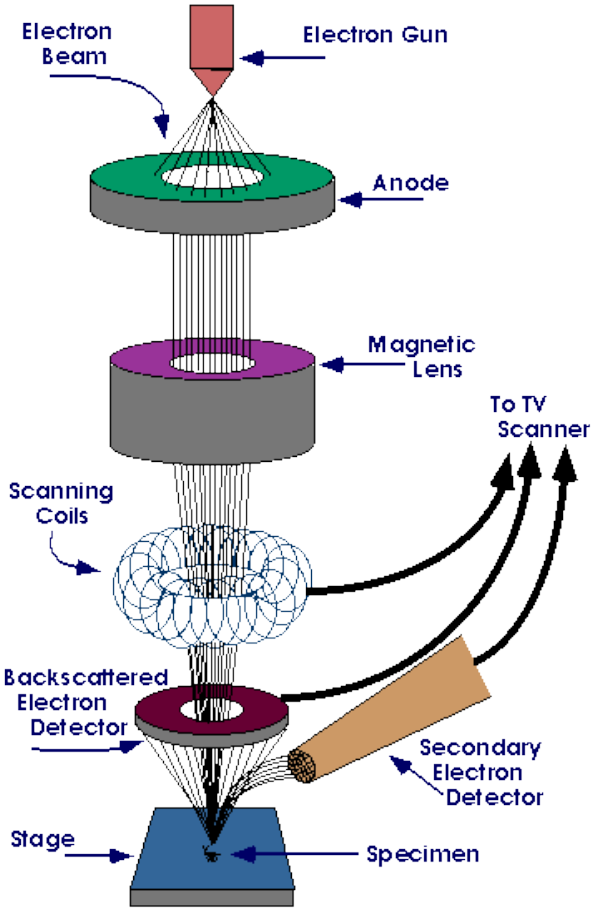

Figure 2.4 Typical diagram of SEM

The SEM is an instrument that produces a largely magnified image by using electrons instead of light to form an image. A beam of electrons is produced at the top of the microscope by an electron gun. The electron beam follows a vertical path through the microscope, which is held within a vacuum. The beam travels through electromagnetic fields and lenses, which focus the beam down toward the sample. Once the beam hits the sample, electrons and X-rays are ejected from the sample.

Detectors collect these X-rays, backscattered electrons, and secondary electrons and convert them into a signal that is sent to a screen similar to a television screen. This produces the final image [7].

2.1.2.4 Applications

The SEM is routinely used to generate high-resolution images of shapes of objects (SEI) and to show spatial variations in chemical compositions:

- Acquiring elemental maps or spot chemical analyses using EDS.
- Discrimination of phases based on mean atomic number (commonly related to relative density) using BSE.
- Compositional maps based on differences in trace element "activators" (typically transition metal and Rare Earth elements) using CL.
- The SEM is also widely used to identify phases based on qualitative chemical analysis and/or crystalline structure**.**

2.1.2.5 Strengths

- Most SEM's are comparatively easy to operate, with user-friendly "intuitive" interfaces.
- Many applications require minimal sample preparation.
- For many applications, data acquisition is rapid (less than 5 minutes/image for SEI, BSE, spot EDS analyses.)
- Modern SEMs generate data in digital formats, which are highly portable.

2.1.2.6 Limitations

- Samples must be solid and they must fit into the microscope chamber.
- Maximum size in horizontal dimensions is usually on the order of 10 cm, vertical dimensions are generally much more limited and rarely exceed 40 mm.
- For most instruments samples must be stable in a vacuum on the order of 10^{-5} - 10^{-6} torr [7].

2.1.3 Energy Dispersive X-Ray Analysis (EDX)

Energy Dispersive X-Ray Analysis (EDX), referred to as EDS or EDAX, is an x-ray technique used to identify the elemental composition of materials. Applications include materials and product research, troubleshooting, deformulation, and more. EDX systems are attachments to Electron Microscopy instruments (Scanning Electron Microscopy (SEM) or Transmission

Electron Microscopy (TEM)) instruments where the imaging capability of the microscope identifies the specimen of interest. The data generated by EDX analysis consist of spectra showing peaks corresponding to the elements making up the true composition of the sample being analyzed. Elemental mapping of a sample and image analysis are also possible. In a multi-technique approach EDX becomes very powerful, particularly in contamination analysis and industrial forensic science investigations. The technique can be qualitative, semi-quantitative, quantitative and also provide spatial distribution of elements through mapping. The EDX technique is non-destructive and specimens of interest can be examined in situ with little or no sample preparation. In situations where combined Microscopy and EDX data acquired are insufficient to identify a specimen, complementary techniques are available, typically Infra-red (FTIR) Microscopy, RAMAN Microscopy, Nuclear Magnetic Resonance Spectroscopy (NMR) and Surface Analysis (X-ray photoelectron spectroscopy (XPS) or Time-of-Flight Secondary Ion Mass Spectrometry (SIMS)) [8].

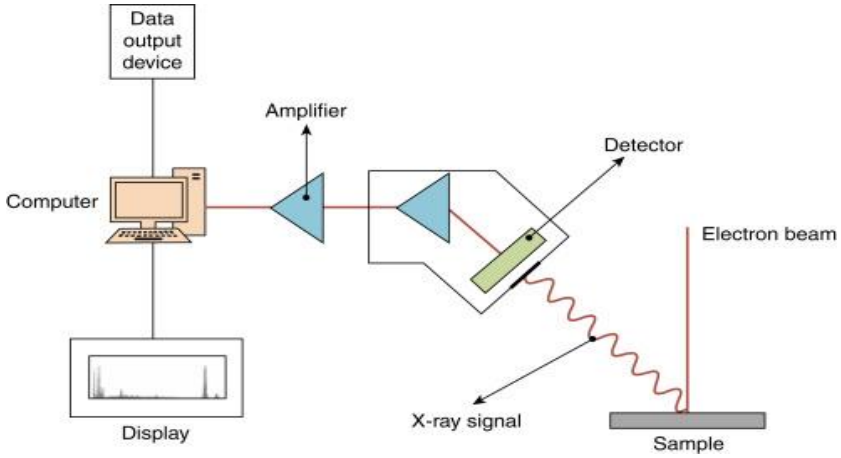

Figure 2.5: Schematic describing the EDX Spectroscopy method

2.1.3.1 Principle

A typical set up of the EDAX is similar with that of SEM set up. More specifically, EDAX is actually inbuilt within the SEM set up. The working of EDX is based on electron focusing same as in SEM. Electron beam excitation is employed in SEM and scanning transmission electron microscopes (STEM) whereas the X-ray beam excitation is present in X-ray fluorescence (XRF) spectrometers. A detector converts X-rays into voltage signals; which feed a pulse processor, to measure the signals and pass them to data analyzer for display and investigation. Si(Li) detector

cooled at cryogenic temperatures by liquid nitrogen is often employed; additionally, some modern systems come with silicon drift detectors (SDD) employing Peltier cooling systems. To produce characteristic X-rays from an object, it is bombarded by either a highly energetic beam of charge carriers (electrons or protons) or X-rays. The atoms of the sample contain ground state (unexcited) electrons in discrete energy levels or electron shells bound to the nucleus. An electron from an inner shell may be excited by an incident beam, thereby removing it from its shell and generating a hole where electron was present before excitation. This hole can be occupied by an electron of a higher-energy shell. The difference in energies of the higher- and lower- energy shells is emitted as an X-ray. Quantitative measurement of the energy and number of these X-rays can be done with energy-dispersive analysis of X-rays. Since the energy of these X-rays is characteristic feature of energy difference between two shells and atomic structure of discharging element, EDAX can be employed to identify the elemental composition of an object [9].

2.1.3.2 Instrumentation

Figure 2.6 shows the working arrangement of EDS with SEM. This instrument is mainly composed of four components:

- Electron beam source
- X−ray Detector
- Pulse Processor
- Analyzer

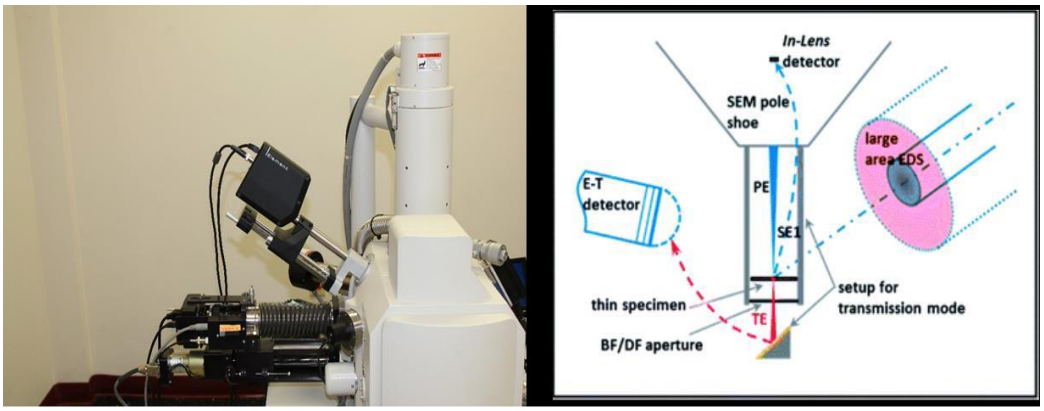

Figure 2.6 Working arrangement of EDAX (Energy dispersive analysis of X−rays)

Brief Description of Components-

- **Electron beam source:** As EDS is employed with the scanning electron microscope therefore the same electron gun (Field Emission) is used as the incident electron source and to focus the beam lenses are used along with aperture. The energy of the electron beam has to be carefully selected to overcome the compromise between the resolution requirements and the production efficiency of X-rays. The produced X-rays are detected by two crystal spectrometers.
- **X−ray Detector:** The X-rays counts (which is the abundance of emitted X-rays) versus X-rays energies are measured by the EDS detector. Detector, a solid state device which is based on lithium drifted silicon. As X−rays strike the surface of the detector, a charge pulse is created. This charge pulse is directly proportional to the energy of the incident X−ray.
- **Pulse Processor:** A charge sensitive preamplifier is employed to convert the charge pulse to a voltage pulse**.**
- **Analyzer:** Multi-channel analyser is used to sort pulses by voltage in the signals which are received by the analyser. The energy of the X-ray can be obtained by measuring the voltage of the charge pulses. This energy is then sent for display and data processing. Here, data is displayed as histogram of intensity vs voltage [9].

2.1.3.3 Working

With an SEM, a variety of signals offer up different information about a given sample. For example, backscattered electrons produce images with contrast that carry information about the differences in the atomic number, while secondary electrons produce topographic information about the sample. Yet when SEM is joined with an EDX detector, X-rays can also be used as a signal to produce chemical information.To understand how these X-rays are generated, it's important to consider that every atom has a unique number of electrons that reside in specific energy levels. Under normal conditions, these positions belong to certain shells, which have different, discrete energy.The way EDX analysis works is that the electron beam hits the inner shell of an atom, knocking off an electron from the shell, while leaving a positively charged electron hole. When the electron is displaced, it attracts another electron from an outer shell to fill the vacancy. As the electron moves from the outer higher-energy to the inner lower-energy

shell of the atom, this energy difference can be released in the form of an X-ray. The energy of this X-ray is unique to the specific element and transition [10].

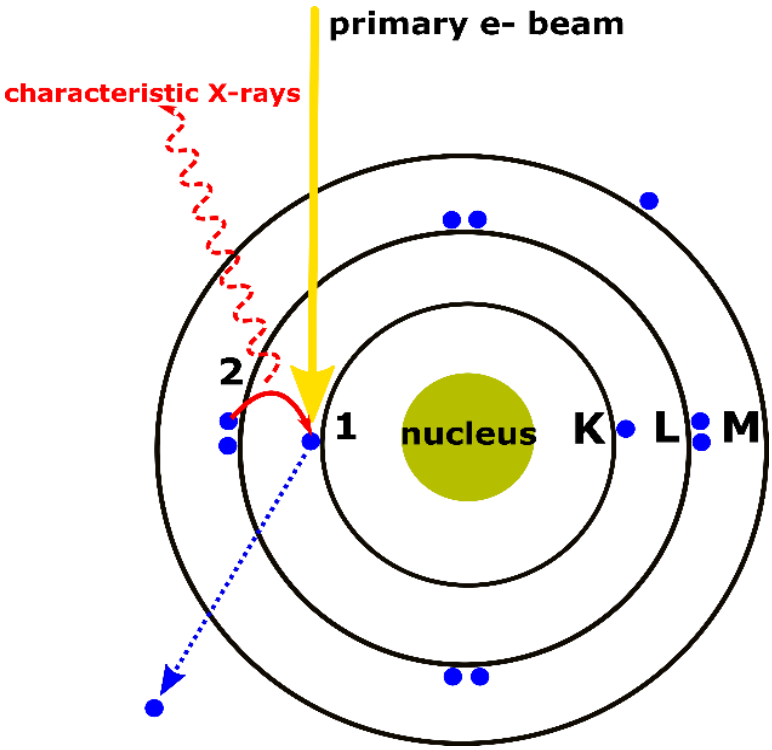

Fig 2.7:X-rays are generated using EDX following a two-step process. First, the energy transferred to the atomic electron knocks it off, leaving behind a hole. Second, its position is filled by another electron from a higher energy shell, and the characteristic X-ray is released.

The X-rays emitted during the process are collected by a silicon drift detector, which measures the signal and interprets it using software. In essence, the chemical information can be visualized in several ways including elemental mapping and line scans. In this way, X-rays can be used to identify each element that exists in a sample. Interestingly, EDX can be used for both qualitative and quantitative analysis, enabling users to identify both the type of elements that are present as well as the percentage of each element's concentration within the sample. And as with traditional SEM, the technique requires little to no sample preparation and is non-destructive, meaning that it doesn't damage the sample. Because of its many advantages, EDX analysis has become common practice across industries ranging from manufacturing or research to energy and resource management to consumer-packaged goods. In fact, it's so practical that it's now an

essential part of owning an SEM. Using an SEM to perform EDX analyses, researchers can improve production quality while saving valuable time—all using a very simple experiment.

2.1.3.4 Applications

- Product deformulation and competitor analysis
- Adhesion, bonding, delamination investigations
- Optical appearance, haze and colour problems
- Disputed claim investigations and expert witness
- Failure investigations, identification of cause
- Catalyst quality, poisoning and elemental distribution
- Product imperfections and defect analysis
- Contamination detection, isolations and identification
- Quality control, raw material and end product
- Filler, pigment, fibre, additive distribution, orientation
- Assessment of plant particulate emissions
- Construction and maintenance monitoring (asbestos) [8]

2.1.3.5 Advantages

It is a relatively quick elemental analysis technique (in most cases); elemental coverage for all but the lightest elements (carbon and above are detectable, boron is problematic); quantitative elemental data; the ability to scan areas (raster scanning) and single spots; a large spatial range from about 1 mm^2 to $submicron^2$; elemental spectra are linked to image data generated by electron microscope; elemental maps, "dot maps," can be generated from the data; depth information is possible using variable excitation voltages and modeling packages such as Monte Carlo simulations; generated data are from only the top couple of microns of the material under investigation (surface sensitive); while many consider this a destructive technique, particularly in the case of electronic components, it is in fact not in many cases (e.g., in most cases electronic components are not damaged by the electron beam) [11].

2.1.3.6 Disadvantages

Because of the most common detector designs, nitrogen produces a very weak response making its detection unreliable for most materials; generated data are from only the top couple of microns of the material under investigation complicating bulk analyses; it is a relatively insensitive method with lower detection limits in the percentage range; only elemental data is generated; quantitative analysis of heterogonous materials often results in inaccurate data; samples must be submitted to vacuum conditions; chamber dimensions often limit the size of samples which may be analyzed (large chamber systems do get around this limitation but are the exception, not the rule); nonconductive samples may need to be coated with a conductive film usually resulting in the analysis being destructive [11].

2.1.4 UV-Visible Spectroscopy

UV spectroscopy is type of absorption spectroscopy in which light of ultra-violet region (200-400nm) is absorbed by the molecule which results in the excitation of the electrons from the ground state to higher energy state.

Nanoparticles have optical properties that are sensitive to size, shape, concentration, agglomeration state, and refractive index near the nano particle surface, which makes UV/Vis/IR spectroscopy a valuable tool for identifying, characterizing, and studying these materials. Standard UV-Vis analysis is performed with an agilent 8453 single beam diode array spectrometer, which collects spectra from 200-1100 nm using a slit width 1nm. Deuterium and tungsten lamps are used to provide illumination across the ultra violet electromagnetic spectrum. Spectra are typically collected from 1ml of a sample dispersion, but we can tests volumes as small as 100microlitre using a microcell with a path length of 1cm.

.

Figure 2.8 UV-VIS Spectrometer

2.1.4.1 Transmittance and Absorbance

The transmittance of a sample(T) is defined as the fraction of photons that pass through the sample over the incident number of photons, i.e.,

$$T=I/I0$$

In a typical UV/Vis spectroscopy measurement, we are measuring those photons that are not absorbed or scattered by the sample. It is common to report the absorbance (A) of the sample, which is related to the transmittance by

$$A=-\log10(T)$$

The relative percentage of scatter or absorption from the measured extinction spectrum depends on the size, shape, composition, and aggregation states of the sample. The sample may absorb light, scatter light, or both. As a general rule, smear particle will have a higher percentage of their extinction due to absorption.

2.1.4.2 Principle

Basically, spectroscopy is related to the interaction of light with matter. As light is absorbed by matter, the result is an increase in the energy content of the atoms or molecules. When ultraviolet radiations are absorbed, this results in the excitation of the electrons from the ground state

towards a higher energy state. Molecules containing π-electrons or non-bonding electrons (n-electrons) can absorb energy in the form of ultraviolet light to excite these electrons to higher anti-bonding molecular orbitals. The more easily excited the electrons, the longer the wavelength of light it can absorb. The absorption of ultraviolet light by a chemical compound will produce a distinct spectrum which aids in the identification of the compound.

2.1.4.3 Instrumentation

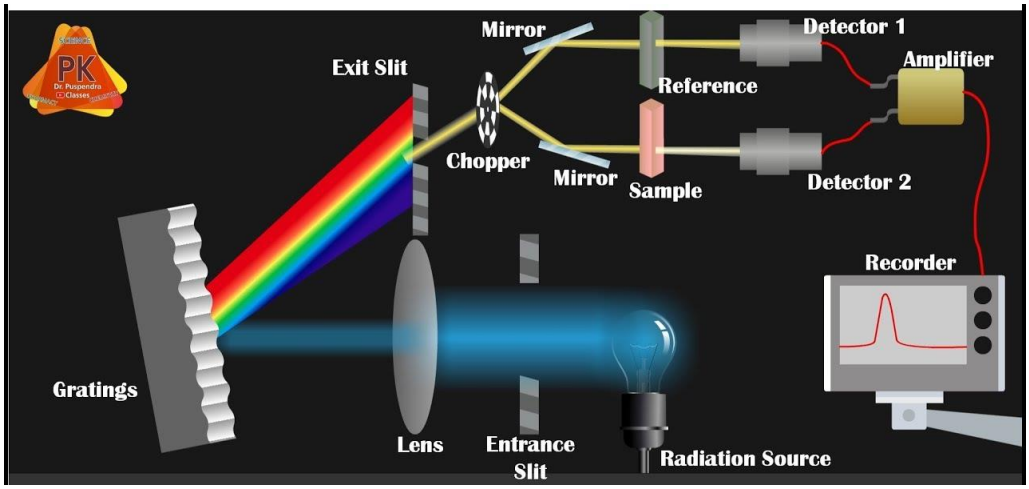

Figure2.9 Working of U-V Spectroscopy

Light Source

Tungsten filament lamps and Hydrogen-Deuterium lamps are most widely used and suitable light source as they cover the whole UV region. Tungsten filament lamps are rich in red radiations; more specifically they emit the radiations of 375 nm, while the intensity of Hydrogen-Deuterium lamps falls below 375 nm.

Monochromator

Monochromators generally is composed of prisms and slits. Most of the spectrophotometers are double beam spectrophotometers. The radiation emitted from the primary source is dispersed with the help of rotating prisms. The various wavelengths of the light source which are separated by the prism are then selected by the slits such the rotation of the prism results ina series of continuously increasing wavelength to pass through the slits for recording purpose. The beam

selected by the slit is monochromatic and further divided into two beams with the help of another prism.

Sample and reference cells

One of the two divided beams is passed through the sample solution and second beam is passé through the reference solution. Both sample and reference solution are contained in the cells. These cells are made of either silica or quartz. Glass can't be used for the cells as it also absorbs light in the UV region.

Detector

Generally, two photocells serve the purpose of detector in UV spectroscopy. One of the photo-cell receives the beam from sample cell and second detector receives the beam from the reference. The intensity of the radiation from the reference cell is stronger than the beam of sample cell. This results in the generation of pulsating or alternating currents in the photocells.

Amplifier

The alternating current generated in the photocells is transferred to the amplifier. The amplifier is coupled to a small servo-meter. Generally current generated in the photocells is of very low intensity, the main purpose of amplifier is to amplify the signals many times so we can get clear and recordable signals.

Recording devices

Most of the time amplifier is coupled to a pen recorder which is connected to the computer. Computer stores all the data generated and produces the spectrum of the desired compound.

2.1.4.4 Applications

- It is one of the best methods for determination of impurities in organic molecules.
- Additional peaks can be observed due to impurities in the sample and it can be compared with that of standard raw material.

- It is useful in the structure elucidation of organic molecules, such as in detecting the presence or absence of UNSATURATION, the presence of hetero atoms.
- UV absorption spectroscopy can be used for the quantitative determination of compounds that absorb UV radiation [12].

❖ **Tauc Plot Method**

The tauc method of optical absorption edge determination as applied specifically to direct bandgap material. A misuse of the tauc plot to determine the bandgap energy of semi-conductors may lead to erroneous estimates, particularly large errors can be associated with characterization of modified semi-conductors showing a significant absorption of sub bandgap energy photon. The bandgap energy of a semi-conductor describes the energy needed to excite an electron from the valence band to the conduction band. We determine the bandgap by plotting [(F(r) hν)2 vs hν] , where hν is the photon energy and F(r) is the (kubelka-munk) K-M function , thus extrapolating these regions we get the energy of the optical bandgap of the material.

So, with the help of DRS we calculate the bandgap with the help of K-M function.

$$(\boldsymbol{r}) = \boldsymbol{k}/\boldsymbol{s}, \ldots\ldots\ldots\ldots\ldots\ldots(5)$$

where k is the molar absorption co-efficient, k= (1-R)^2, R is the Reflectance.

S is the scattering factor, S=2R

The photon energy hν can be calculated using the equation,

$$\boldsymbol{h\nu} = \mathbf{1240}/\boldsymbol{wavelength}\ldots\ldots\ldots\ldots\ldots\ldots(6)$$

the tauc method uses simple multi-wavelength absorption spectroscopy and is relied upon for material evaluation of functional photovoltaic layers, transparent conductors, sensor coatings and films used for many other applications [13].

2.1.5 Raman Spectroscopy

Raman Spectroscopy is a non-destructive chemical analysis technique which provides detailed information about chemical structure, phase and polymorphy, crystallinity and molecular interactions. It is based upon the interaction of light with the chemical bonds within a material.

Raman is a light scattering technique, whereby a molecule scatters incident light from a high intensity laser light source. Most of the scattered light is at the same wavelength (or color) as the laser source and does not provide useful information – this is called Rayleigh Scatter. However a small amount of light (typically 0.0000001%) is scattered at different wavelengths (or colors), which depend on the chemical structure of the analyte – this is called Raman Scatter. A Raman spectrum features a number of peaks, showing the intensity and wavelength position of the Raman scattered light. Each peak corresponds to a specific molecular bond vibration, including individual bonds such as C-C, C=C, N-O, C-H etc., and groups of bonds such as benzene ring breathing mode, polymer chain vibrations, lattice modes, etc [13].

When light interacts with molecules in a gas, liquid, or solid, the vast majority of the photons are dispersed or scattered at the same energy as the incident photons. This is described as elastic scattering, or Rayleigh scattering. A small number of these photons, approximately 1 photon in 10 million will scatter at a different frequency than the incident photon. This process is called inelastic scattering, or the Raman effect, named after Sir C.V. Raman who discovered this and was awarded the 1930 Nobel Prize in Physics for his work. Since that time, Raman has been utilized for a vast array of applications from medical diagnostics to material science and reaction analysis. Raman allows the user to collect the vibrational signature of a molecule, giving insight into how it is put together, as well as how it interacts with other molecules around it [13].

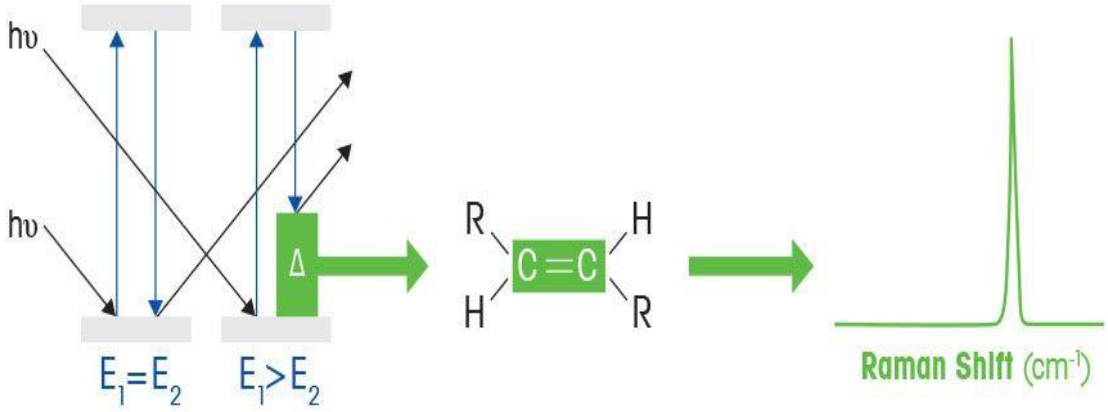

Fig 2.10 Raman spectroscopy

2.1.5.1 Raman Scattering Process

The Raman Scattering Process, as described by quantum mechanics, is when photons interact with a molecule, the molecule may be advanced to a higher energy, virtual state. From this higher energy state, there may be a few different outcomes. One such outcome would be that the molecule relaxes to a vibrational energy level that is different than that of its beginning state producing a photon of different energy. The difference between the energy of the incident photon and the energy of the scattered photon is the called the Raman shift. When the change in energy of the scattered photon is less than the incident photon, the scattering is called Stokes scatter. Some molecules may begin in a vibrationally excited state and when they are advanced to the higher energy virtual state, they may relax to a final energy state that is lower than that of the initial excited state. This scattering is called anti-Stokes [14].

2.1.5.2 Instrumentation

A modern, compact Raman spectrometer consists of several basic components, including a laser that serves as the excitation source to induce the Raman scattering. Typically, solid state lasers are used in modern Raman instruments with popular wavelengths of 532 nm, 785 nm, 830 nm and 1064 nm. The shorter wavelength lasers have higher Raman scattering cross-sections so the resulting signal is greater, however the incidence of fluorescence also increases at shorter wavelength. For this reason, many Raman systems feature the 785 nm laser. The laser energy is transmitted to and collected from the sample by fiber optics cables. A notch or edge filter is used to eliminate Rayleigh and anti-Stokes scattering and the remaining Stokes scattered light is passed on to a dispersion element, typically a holographic grating. A CCD detector captures the light, resulting in the Raman spectrum. Since Raman scattering yields a weak signal, it is most important that high-quality, optically well-matched components are used in the Raman spectrometer [14].

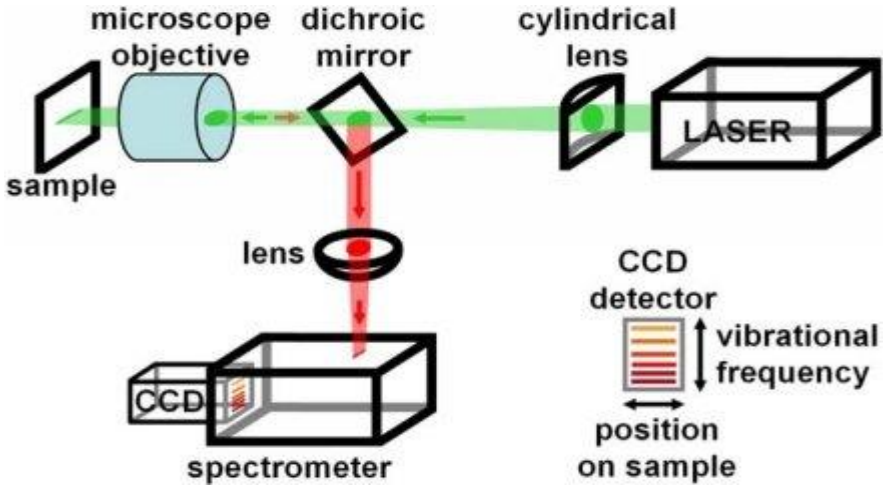

Figure 2.11 Raman Spectrometer

2.1.5.3 Applications

Raman spectroscopy is used in industry for a variety of applications, including:

- Crystallization Processes
- Polymorphism Identification
- Polymerization Reactions
- Hydrogenation Reactions
- Chemical Synthesis
- Biocatalysis and Enzymatic Catalysis
- Flow Chemistry
- Bioprocess Monitoring
- Synthesis Reactions [14]

2.1.5.4 Advantages

- Chemical composition and structure of materials**.**
- Non-contacting and non-destructive**.**
- Sample preparation is not needed.
- You can choose how much, or little, of the sample you want to analyze
- Analyze through transparent containers and windows
- Sensitive to small changes in material structure

- Can analyze samples in water

2.1.5.5 Disadvantages

- Cannot be used for metals or alloys.
  - the Raman effect is very weak. The detection needs a sensitive and highly optimized instrumentation.
  - fluorescence of impurities or of the sample itself can hide the Raman spectrum. Some compounds fluoresce when irradiated by the laser beam.
  - sample heating through the intense laser radiation can destroy the sample or cover the Raman spectrum [15].

2.1.6 Fourier Transform Infrared Spectroscopy (FTIR)

The FTIR instrument is one of the most important tools to identify the chemical components that are either organic (or) inorganic compounds presence in the synthesized materials. The FTIR analysis was used to find out the presence of various functional groups presence in the prepared sample which was taken in solid and liquid state using Perkin-Elmer spectrometer in the range of 400-4000 cm-1.

2.1.6.1 Physical Principles

Various frequencies, molecular bonds are vibrating owing to their elements and bonds presence in the synthesized material. According to the quantum mechanics, several specific frequencies were vibrating such as ground state at lowest frequency and several excited states at higher frequencies. If the frequency of a molecular vibration linearly increases, the light energy will be absorbed, which may happen by the difference between two energy states (ground state (E0) – first excited state (E1)) and the relation is given below,

$$E1 - E0 = hc/\lambda \quad \text{..... (3)}$$

Where:

h represents the Planck's constant.

c denotes the velocity of the light.

λ is the wavelength of light.

2.1.6.2 Experimental

The figure below shows the basic set up of the FTIR spectrometer. The FTIR spectrometer has following parameters such as (i) interferometer which consist of two mirrors such as infrared detector and beam splitter, (ii) detector, (iii) monochromator and (iv) chopper. In the FTIR studies, both solid and liquid samples were used to analysis. The KBr (or) polyethylene pellets were used to take the solid and liquid sample in FTIR analysis. For solid sample, few milligrams of the prepared samples are mixed with the KBr and fine grain in the mortar. After that the fine powder was pressed with the hydraulic pressure to make the pellet. Finally, the pellet sample was fixed with sample holder to take the FTIR analysis. For liquid sample, few drops of the samples were dropped into pure KBr pellet and few minutes dried the pellet at room temperature. After that the pellet was used to FTIR characterization.

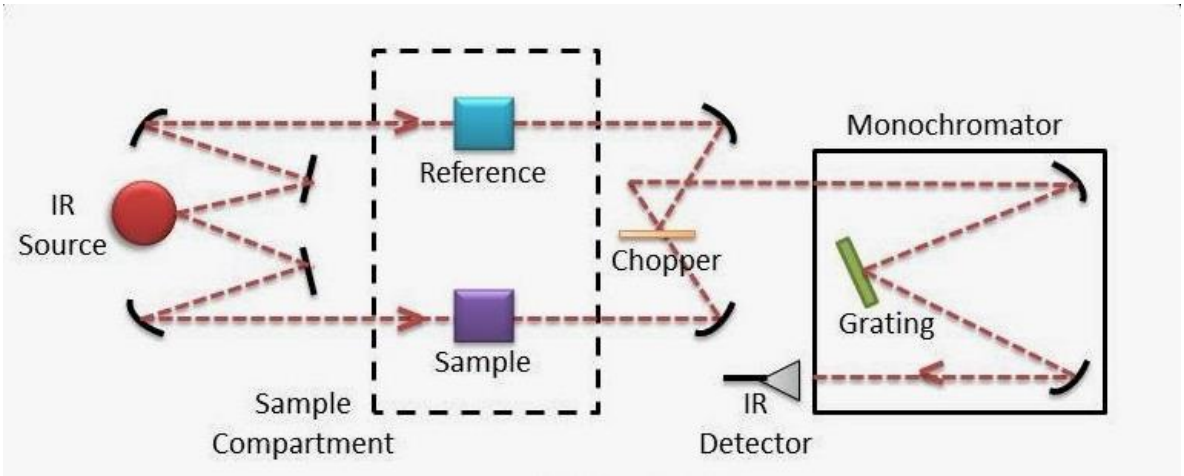

Figure 2.12 FTIR instrument setup

2.1.6.3 Applications

- Quality verification of incoming/outgoing materials
- Deformulation of polymers, rubbers, and other materials through thermogravimetric infra-red (TGA-IR) or gas chromatography infra-red (GC-IR) analysis

- Microanalysis of small sections of materials to identify contaminants
- Analysis of thin films and coatings
- Monitoring of automotive or smokestack emissions
- Failure analysis [16]

2.1.6.4 Strengths

- Highly sensitive and quick method to achieve high quality spectrum.
- This spectroscopy gives better signal to noise ratio compared to the dispersive instrument.
- Gases, solids as well as liquid can be analysed with FTIR.
- By using FTIR no external calibration is required and gives accurate results.
- Organic compounds and Inorganic compounds can be identified easily using fourier transform infrared spectroscopy.
- Simultaneous analysis can be done for multiple gaseous compounds.
- FTIR can identify even small concentrations of contaminants.
- FTIR has a laser beam which keeps the FTIR instrument accurately calibrated.
- High resolution [17]**.**

2.1.6.5 Limitations

- The sampling chamber of an FTIR can present some limitations due to its relatively small size.
- Mounted pieces can obstruct the IR beam. Usually, only small items as rings can be tested.

Several materials completely absorb Infrared radiation; consequently, it may be impossible to get a reliable result [18].

Reference

[1] Indian Journal of Fiber &textile Research Vol 33, September 2008,pp 304-317

[2] G. R. Chatwal, S. K. Anand, Instrumental methods of chemical analysis, Himalaya publishing house Mumbai, 1979.

[3] C. Suryanarayana, M. G. Norton, X-ray diffraction: a practical approach, 207; 1998.

[4] Y. Waseda, E. Matsubara, K. Shinoda, X-ray diffraction crystallography: introduction, examples and solved problems, Springer Science & Business Media, 2011.

[5] https://serc.carleton.edu/research_education/geochemsheets/techniques/XRD.html

[6] https://serc.carleton.edu/research_education/geochemsheets/techniques/SEM.html

[7] https://www.purdue.edu/ehps/rem/laboratory/equipment%20safety/Research%20 Equipment/sem.html

[8] https://www.intertek.com/analysis/microscopy/edx/

[9] 1585214200-PHY(H) -VI-NANO-MATERIAL-1-AJAYPRADAP. pdf

[10] Thermofisher.com/blog/microscopy/edx-analysis-wirh-sem-how-does-it-work/

[11] Science direct. com/topics/chemistry/energy-dispersive-spectroscopy

[12] https:// microbenotos. com/uv-spectroscopy-principle-instrumentation-application

[13] Evaluation of taue method for optical absorption edge determination:ZnO Thin films as a model system. Viezbicke, Brain D;Patel Shane ; Davis, Benjamin E:et.al

[14] https://www.horiba.com/pol/scientific/technologies/raman- imaging-and spectroscopy /raman-spectroscopy/

[15]mt.com/in/en/home/applications/Raman spectroscopy. Html

[16] rds.ro/blog/articles/advantages-disadvantages-raman spectroscopy/

[17] https://www.thermofisher.com/in/en/home/industrial/spectroscopy-elemental-isotope-analysis/spectroscopy-elemental-isotope-analysis-learning-center/molecular-spectroscopy-information/ftir-information/ftir applications. html#:~:text=Some%20of%20 the%20more%20 common,of%20materials%20to%20identify%20contaminants

[18] https://www.pharmastuff4u.com/2014/06/advantages-and-disadvantages-of-ftir.html

[19] https://agta.org/advantages-and-disadvantages-of-raman-fourier-transform-infrared-spectroscopy-ftir-in-the-gemological-field/

CHAPTER 3

SYNTHESIS METHOD

3.0 Synthesis Of Nanoparticles

Zinc oxide is considered to be a technologically prodigious material having a wide spectrum of applications such as that of a semiconductor, magnetic material, nanostructure varistor, thermo electric material, gas sensor, constituent of cosmetics etc. there are several synthesis procedures for the preparation of ultraline oxide nanoparticles such as sol-gel, spray pyrolysis, chemical vapour deposition, precipitation method, hydrothermal method etc. here we use hydrothermal method for the preparation of Zno material. The main parameters of hydrothermal synthesis which define both the processes kinetics and the properties of resulting products, are the initial pH of the medium, the duration and temperature of synthesis and the pressure in the system.[1]

3.1 Synthesis Procedure

Zinc acetate hexahydrate ($Zn(CH_3CO_2)_{2.}2H_2O$), Nickel nitrate ($Ni(NO_3)_2.6H_2O$) (Sigma Aldrich, 99.9%purity) are used as the precursors. All the raw chemicals are also purchased from Merck.

0.5 g of Zinc acetate hexahydrate ($Zn(CH_3CO_2)_{2.}2H_2O$)taken and dissolved in 40 ml distilled water. The solution is kept under stirring until the solution is become homogeneous. To the above solution Ammonia solution is added drop wise drop to maintain the pH approximately 11 and again stirring is continued for an hour. Finally, the above solution is transferred to 100 ml Teflon beaker. Then Teflon beaker is kept in autoclave which is placed in hydrothermal oven for 150^0 c for 4 hrs. After the autoclave is naturally cool down we can collect the precipitate by centrifugation. The collected particles then kept for drying at 80 ^{0} C for 12 hrs in an oven. Then particles are grinded well to make fine powder. The procedure can be repeated for doped samples. For the doping the required amount of Ni can be added along with zinc precursor and following the same procedure.

References:

1. https://www.ncbi.nlm.nih.gov/pmc/articles/PMC5453364/

CHAPTER 4

RESULT AND DISCUSSION

4.1 Xrd

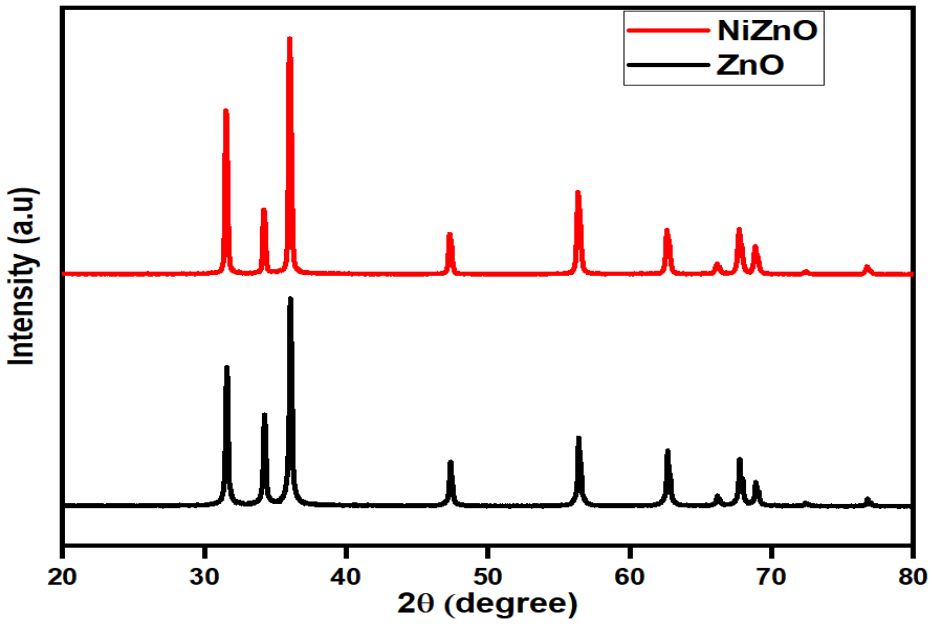

Figure 4.1 XRD patterns of hydrothermally synthesized ZnO and Ni-Zn

The phase purity and crystalline nature of pure and Ni-doped ZnO nanostructures were investigated using powder X-ray diffraction analysis, as shown in the fig 4.1. XRD pattern shows peaks at 2θ = 31.77°, 34.43°, 36.26°, 47.55°, 56.60° , 62.87°, 66.38°, 67.96°, 69.08°, 72.59° and 76.97° corresponding to (100), (002), (101), (102), (110), (103), (200), (112), (201), (004) and (202) planes respectively and are in perfect agreement with standard JCPDS data (card no.89 – 0510). The XRD results reveals the hexagonal wurtzite structure having $P6_3mc$ space group [1]. All the diffraction peaks of synthesized samples were assigned to zinc oxide and no extra impurity peaks were identified within the instrumental detection limit [2]. This indicate that the nickel dopant is incorporated to the lattice site of zinc oxide without distorting its crystal symmetry[3]. The average crystallite size of pristine and Ni doped ZnO nanostructures were obtained from the Debye-Scherrer formula and is tabulated in table 1

$$D = \frac{k\,\lambda}{\beta \cos\theta} \text{.....(8)}$$

Sample code	a(Å)	Crystallite Size (nm)
ZnO	3.2493	37.3089
2.5NiZnO	3.2488	31.2099

Table 1: Crystalline Size of ZnO and Ni-ZnO

4.2 SEM & EDAX

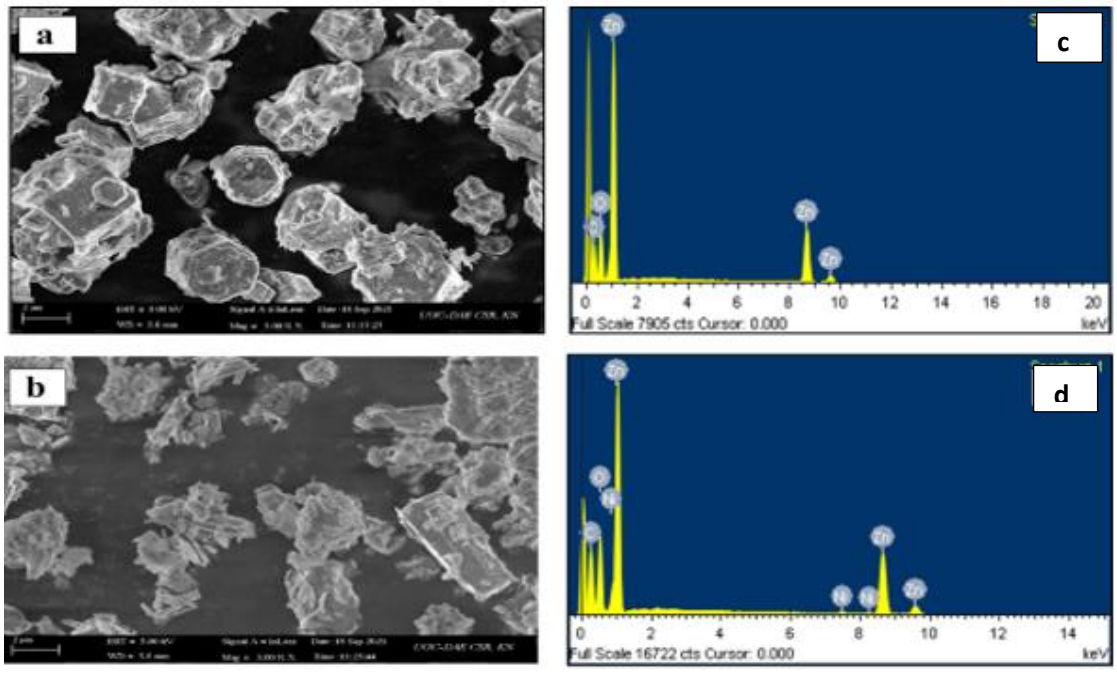

Figure 4.2(a)&(b) Sem imahe of pure and Ni doped ZnO,(c) &(d) Edax spectra of ZnO and Ni-ZnO.

Morphology of the synthesized sample can be observed from the SEM image as shown in fig4.2. From the image 4.2:(a) it is clear that pure ZnO shows a distorted rod like structure with smaller particle size [4]. With the incorporation of Ni, the particle size changes into larger from the pure ZnO due to the gradual increase in grain growth. Thus, the presence of Ni significantly influences the morphology of ZnO nanostructures and can conclude that the addition of Ni effectively changes the surface morphological characteristics of pure ZnO.

Fig 4.2:(b) reveals the EDAX spectra of pristine and Ni doped ZnO. The EDAX spectra of ZnO reveals the presence of zinc and oxygen having atomic weight % of 46.23% and 23.17 % respectively. EDAX spectrum for Ni doped ZnO also confirms the occurrence of Zinc, Nickel and Oxygen.Ni doped ZnO contains 39.34% of Zn, 26.54% of O and 0.41% of Ni.

4.3 UV visible Spectroscopy

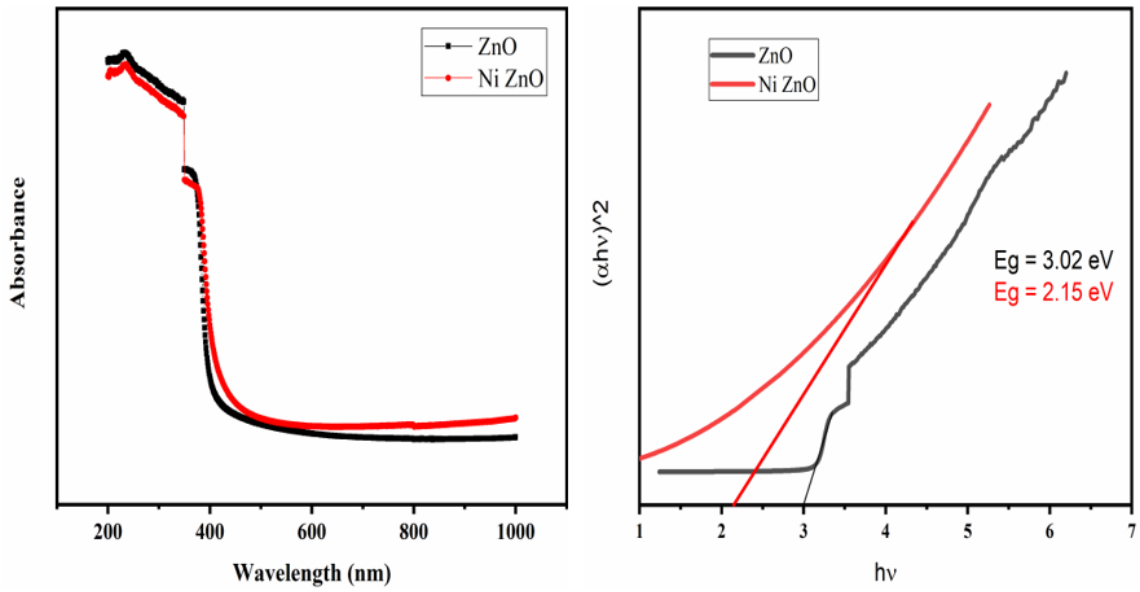

(a) **(b)**

Figure 4.3 (a) The UV curve of pure and doped Ni-ZnO and **(b)**Tauc plot of pure and doped Ni-ZnO.

The linear optical characteristics of undoped and doped nanostructures were investigated by UV-Visible DRS spectra for the spectral limit 200-1000 nm. The absorption curve of synthesized nanostructures exhibits a strong absorption around 340-375 nm as shown in figure 4.3(a). [5].

Generally, absorbance value relates on the surface roughness, band gap, oxygen deficiency and impurity points on the samples. For Ni doped ZnO the absorbance edge was shifted to the higher energy level [6]. Fig 4.3(a) depicts the absorbance curve of synthesized nanostructures. The optical band gap (E_g) of prepared nanostructures determined using absorbance spectra using tauc plot method given in the Fig 4.3(b).

Since, ZnO is a direct bandgap semiconductor which shows a linear behavior just above its absorption edge, Eg can be evaluated by extrapolating the linear region of $[\alpha.h\nu]^2$ to the $h\nu$ axis as shown in Fig 4.3(b).The direct bandgap is determined as 3.02 eV, 2.15 eV for undoped , and Ni doped Zno respectively. The observed decrease in bandgap for doped one is ascribed to strong sp – d exchange interaction with both band electrons as well as d electrons of doped Ni^{2+} cations. Decrease in bandgap energy might be the creation of defects on energy level of Ni. Doping with Ni, reduces the bandgap of ZnO by acting like a donor impurity which creates a narrow donor state just below the conduction band (CB).

Sample code	**Band gap energy (eV)**
ZnO	3.02
2.5 %Ni ZnO	2.15

Table 2 Band gap energy of of pure and doped Ni-ZnO**.**

4.4 Ftir and Raman Spectroscopy

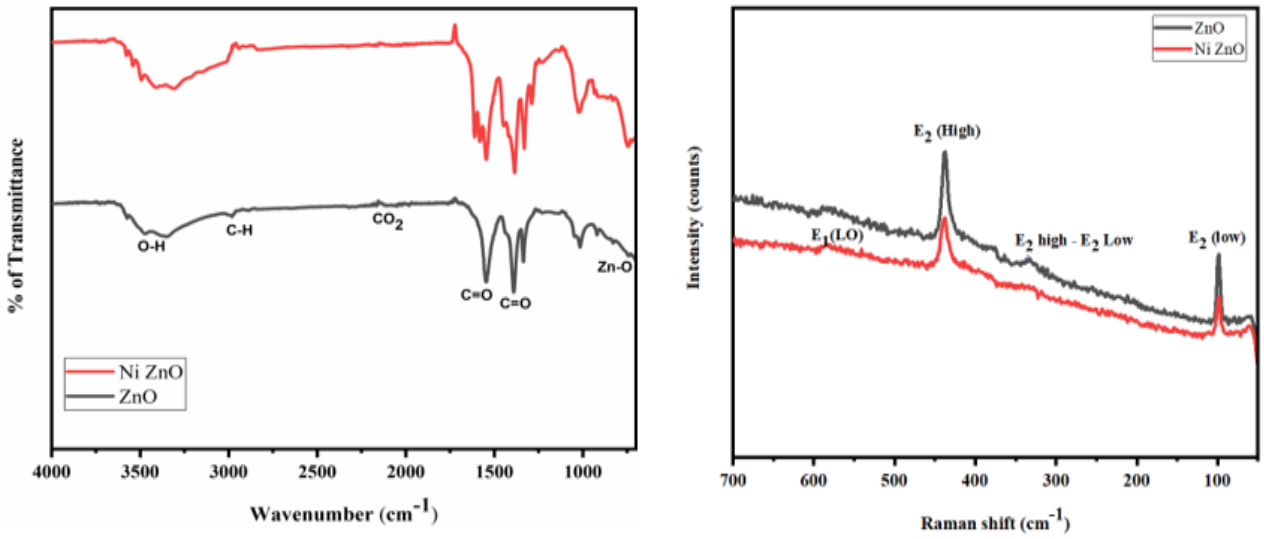

Figure 4.4(a) the FT-IR spectrum of pure and doped ZnO and **(b)** the Raman spectra of pure and doped ZnO

Vibrational spectral studies of Pristine and doped nanostructures were analyzed using FT-IR and micro- Raman spectroscopy. The FT-IR spectroscopy provides information regarding vibrational frequencies, stretching modes, chemical bonding and elemental constituents of synthesized samples. Fig 4.4(a) shows the FT-IR spectrum of pure and doped within a region of 4000 - 500 cm^{-1}. The broad band observed in between 3456 cm^{-1} - 3354 cm^{-1} represents O –H stretching mode [7]. Peak around 1553 cm^{-1} corresponds for O-H bending mode [8]. Vibrational modes presented nearly 1017 cm^{-1} and 672 cm^{-1} are indicates the occupation of Ni^{2+} at Zn^{2+} sites. Stretching band at 667 cm^{-1} are points to the confirmation of rod shaped ZnO. Peaks appeared around 432, 445 and 467 cm^{-1} indicates E_2 mode related to wurtzite structure of pure and doped ZnO respectively [8,9]

Raman spectroscopy were widely used as an important analysis technique to analyze the lattice vibrations, changes in local structure and presence of defects states or disorder in pristine ZnO host lattice due to the influence of nickel ion in its lattice sites [13,10]. Generally, wurtzite type zinc oxide belongs to the space group of $P6_3mc$ having optical phonon modes at its Brillouin zone. In total there exist 12 phonon modes, among which six of them are in transverse optical mode (TO mode), three in longitudinal optical mode (LO mode), two with transverse acoustic mode (TA mode) and one longitudinal acoustic mode (LA mode). Optical phonon modes occurred on Γ point of Brillouin zone is expressed as

$$\boldsymbol{\Gamma_{optical} = A_1 + 2B_1 + E_1 + 2E_2 \ldots\ldots\ldots\ldots (9)}$$

Where, A_1 and E_1 are Raman and IR active polar modes, which can be divided as longitudinal (LO) and transverse (TO) optical phonons, E_2 is a Raman active non-polar mode and B_1 is a Raman inactive mode [10].Fig 4.4(b) shows the Raman spectra of Ni doped ZnO nanostructures on the spectral region of 700 -50 cm^{-1} . Strong peaks nearly about 99-100 cm^{-1} and 436-438 cm^{-1} represents E_2 mode with low (E_2^{low}) and high (E_2^{high}) frequency branches respectively. The E_2^{low} mode arises due to the vibrations of Zn atom, while the E_2^{high} mode is due to motion of O atoms within the lattice sites of ZnO. E_2^{high} mode is the strongest mode in ZnO wurtzite structure and its dominant peak observed at 437 cm^{-1} reveals the presence phase pure wurtzite structure of prepared samples [7]. E_2 high and low modes are more prominent in pristine ZnO and a tremendous reduction in the peak intensity is seen in the Ni doped ZnO nanostructure [7]. This reduction in intensity clearly shows a distortion of parent ZnO lattice due to doping and this indicates the addition of Ni to the Zn host lattice [12]. In pristine ZnO, the peak appeared around 332 cm $^{-1}$ indicates $E_2^{high} - E_2^{low}$ mode corresponding to multiple – phonon scattering process. This vibrational mode is known as Frohlich type vibrational mode and is attributes to single crystalline nature of pristine nanostructures [11]. For Ni doped ZnO nanostructures, two additional peaks are centered around 547 cm $^{-1}$ and 574 cm $^{-1}$ are possibly caused by Ni doping. Peak around 574 cm $^{-1}$ indicates E_1 (LO) mode and ascribed to the defect states due to oxygen vacancies and Zinc interstitials. B. Pal et al. observed similar mode of vibration in Ni doped ZnO synthesized via ball milling method and they found that this additional mode is caused by the lower ionic radii of Ni^{2+} ion as compared to that of Zn^{2+} ions [13]. The table 3 shows the phonon vibrational frequencies and their corresponding assignments. The Raman analysis reveals addition of Ni^{2+} ions to the host lattice of pure ZnO

Raman vibrational frequency (cm $^{-1}$)	**Assignment**
99	E_2^{low}

332	$E_2^{high} - E_2^{low}$
437	E_2^{high}
574	$E_1\ (LO)$

Table 3 Phonon vibrational frequencies and its corresponding assignments

Reference:

1.P. S. Vindhya, T. Jeyasingh, and V. T. Kavitha, "Dielectric properties of zinc oxide nanoparticles using annona muricata leaf," Kerala, India, 2019, p. 080005. doi: 10.1063/1.5093888.

2.C. J, S. N, D. A, and P. D, "Synthesis and Characterization of Ni and Cu Doped ZnO," *J Nanomed Nanotechnol*, vol. 08, no. 02, 2017, doi: 10.4172/2157-7439.1000429.

3.M. Ali *et al.*, "Preparation of Co and Ni doped ZnO nanoparticles served as encouraging nano-catalytic application," *Mater. Res. Express*, vol. 6, no. 12, p. 1250d5, Jan. 2020, doi: 10.1088/2053-1591/ab6383.

4.S. A. Kadam, S. A. Thomas, Y.-R. Ma, L. Maria Jose, D. Sajan, and A. Aravind, "Investigation of adsorption and photocatalytic behavior of manganese doped zinc oxide nanostructures," *Inorganic Chemistry Communications*, vol. 134, p. 108981, Dec. 2021, doi: 10.1016/j.inoche.2021.108981.

5.F. I. H. Rhouma *et al.*, "The structure and photoluminescence of a ZnO phosphor synthesized by the sol gel method under praseodymium doping," *RSC Adv.*, vol. 9, no. 9, pp. 5206–5217, 2019, doi: 10.1039/C8RA09939A.

6.K. Karthika and K. Ravichandran, "Tuning the Microstructural and Magnetic Properties of ZnO Nanopowders through the Simultaneous Doping of Mn and Ni for Biomedical Applications," *Journal of Materials Science & Technology*, vol. 31, no. 11, pp. 1111–1117, Nov. 2015, doi: 10.1016/j.jmst.2015.09.001

7.P. G. Undre, P. B. Kharat, R. V. Kathare, and K. M. Jadhav, "Ferromagnetism in Cu2+ doped ZnO nanoparticles and their physical properties," *J Mater Sci: Mater Electron*, vol. 30, no. 4, pp. 4014–4025, Feb. 2019, doi: 10.1007/s10854-019-00688-4.

8.P. R. Chithira and T. T. John, "Defect and dopant induced room temperature ferromagnetism in Ni doped ZnO nanoparticles," *Journal of Alloys and Compounds*, vol. 766, pp. 572–583, Oct. 2018, doi: 10.1016/j.jallcom.2018.06.336.

9.G. Vijayaprasath, R. Murugan, T. Mahalingam, and G. Ravi, “Comparative study of structural and magnetic properties of transition metal (Co, Ni) doped ZnO nanoparticles,” *J Mater Sci: Mater Electron*, vol. 26, no. 9, pp. 7205–7213, Sep. 2015, doi: 10.1007/s10854-015-3346-z.

10.A. K. Rana, Y. Kumar, P. Rajput, S. N. Jha, D. Bhattacharyya, and P. M. Shirage, “Search for Origin of Room Temperature Ferromagnetism Properties in Ni doped ZnO Nanostructure,” p. 23, 2017.

11.A. Hassanpour, N. Bogdan, J. A. Capobianco, and P. Bianucci, “Hydrothermal selective growth of low aspect ratio isolated ZnO nanorods,” Materials & Design, vol. 119, pp. 464–469, Apr. 2017, doi: 10.1016/j.matdes.2017.01.089.

12.https://www.researchgate.net/publication/280098692_Preparation_structural_photoluminescence_and_magnetic_studies_of_Cu_doped_ZnO_nanoparticles_co-doped_with_Ni_by_sol-gel_method

13.B. Pal, D. Sarkar, and P. K. Giri, “Structural, optical, and magnetic properties of Ni doped ZnO nanoparticles: Correlation of magnetic moment with defect density,” Applied Surface Science, vol. 356, pp. 804–811, Nov. 2015, doi: 10.1016/j.apsusc.2015.08.163.

CHAPTER 5

CONCLUSION & FUTURE SCOPE

In the present work pure and Ni doped ZnO is prepared through hydrothermal method with controlled morphology. The structural, surface morphological Functional groups and vibrational bands of ZnO and Ni doped ZnO have been analyzed using Xrd, Sem, Edax, Ftir and Raman spectroscopy. The phase purity and crystalline nature of pure and Ni-doped ZnO nanostructures were investigated using powder X-ray diffraction analysis. The XRD results reveals the hexagonal wurtzite structure having P63mc space group. All the diffraction peaks of synthesized samples were assigned to zinc oxide and no extra impurity peaks were identified within the instrumental detection limit. This indicate that the nickel dopant is incorporated to the lattice site of zinc oxide without distorting its crystal symmetry. Morphology of the synthesized sample has been observed from the SEM image. From the image it is clear that pure ZnO shows a distorted rod like structure with smaller particle size. With the incorporation of Ni, the particle size changes into larger from the pure ZnO due to the gradual increase in grain growth. Thus the presence of Ni significantly influence the morphology of ZnO nanostructures and can conclude that the addition of Ni effectively changes the surface morphological characteristics of of pure ZnO.The EDAX spectra of ZnO reveals the presence of Zinc, Nickel and Oxygen. It shows the purity of the prepared material as there were no other impurity peaks. The functional groups of prepared sample are identified through FTIR and are similar to that of ZnO. Vibrational bands are identified through Raman and are identical when compared with reported papers. Also the bandgap obtained through UV visiblespectroscopy and which is similar to the reported values.

FUTURE SCOPE

- We can dope with different metal oxides with ZnO using different synthesis methods with different concentrations.The future for high quality Zinc Oxide is certainly going to be fascinating. The potential advances for non-medical applications even surpass that of the current medical uses.
- Making composite with different materials and there by enhancing the properties
- Zinc Oxide nanorod sensors, spintronics, and piezoelectricity are all very promising fields and ones to keep an eye on in the not too distant future.

- Biomedical applications
- Sensor technology is one of the most significant technology for the future with a constantly growing number of applications, ranging from toxic gas detection, manufacturing process monitoring to medical diagnosis and health monitoring. Among the different existing sensor technologies, the semiconductor sensors are most attractive for their high sensitivity, small size and light-weight construction. Additionally, they are cheap, rugged and simple in operation which makes them suitable for a large number of applications.[1]

Reference:

1.https://citeseerx.ist.psu.edu/viewdoc/download?doi=10.1.1.695.6815&rep=rep1&type=pdf